1986

First-principles study of phonon anomalies and the bcc-hcp martensitic phase transition

Yin Chen
Iowa State University

Chen, Yin

FIRST-PRINCIPLES STUDY OF PHONON ANOMALIES AND THE BCC-HCP MARTENSITIC PHASE TRANSITION

Iowa State University PH.D. 1986

PLEASE NOTE:

In all cases this material has been filmed in the best possible way from the available copy. Problems encountered with this document have been identified here with a check mark __✓__.

1. Glossy photographs or pages _____
2. Colored illustrations, paper or print _____
3. Photographs with dark background _____
4. Illustrations are poor copy _____
5. Pages with black marks, not original copy _____
6. Print shows through as there is text on both sides of page _____
7. Indistinct, broken or small print on several pages ✓
8. Print exceeds margin requirements _____
9. Tightly bound copy with print lost in spine _____
10. Computer printout pages with indistinct print _____
11. Page(s) _____ lacking when material received, and not available from school or author.
12. Page(s) _____ seem to be missing in numbering only as text follows.
13. Two pages numbered _____. Text follows.
14. Curling and wrinkled pages _____
15. Dissertation contains pages with print at a slant, filmed as received _____
16. Other _____

_____

_____

University
Microfilms
International

First-principles study of phonon anomalies and the bcc-hcp martensitic phase transition

by

Yin Chen

A Dissertation Submitted to the
Graduate Faculty in Partial Fulfillment of the
Requirements for the Degree of
DOCTOR OF PHILOSOPHY

Department: Physics
Major: Solid State Physics

Approved:

Signature was redacted for privacy.

In Charge of Major Work

Signature was redacted for privacy.

For the Major Department

Signature was redacted for privacy.

For the Graduate College

Iowa State University
Ames, Iowa

1986

TABLE OF CONTENTS

GENERAL INTRODUCTION

Because of the extreme technological importance of phase transitions in solids, there is a large phenomenological approach to the subject.[1,2] A first principles theoretical approach whereby the features of phase transformations could be predicted precisely along with other important physical properties has long been a goal which would lead to materials by design. Progress toward this goal has recently been achieved through the development of accurate methods to calculate the total energy difference associated with atomic displacements in solids. These techniques have been used with great success in first principles studies of lattice vibrations in various crystals via 'frozen phonon' calculations. In addition to giving an accurate description of harmonic forces, these methods also include the anharmonic contributions and thus are inherently more powerful than traditional phonon methods in studying structural phase transitions where a phonon mode goes soft. In this thesis we focus on the bcc-hcp martensitic phase transition and show how the application of these methods can yield new insights into the microscopic interactions governing structural phase transitions.

Martensitic Phase Transition

In terms of broad materials significance the principal types of phase transitions are: liquid-solid, solid-solid compositional separation, and martensitic. The geometrical or structural description

of martensitic transformations is a well developed discipline[1,2], but the underlying microscopic interactions which drive such transformations are less well understood.

Historically the term "martensitic" derives from the studies of Professor A. Martens, a pioneer German metallographer, of quenched iron-carbon steel which has high hardness and fine scale microstructure and is much more useful than slow cooled iron-carbon. Martensite is always a heterogeneous structure (e.g., plates, needles, lenses of a product phase mixed into a parent phase).

The general features of the martensitic transition are:

(a) Parent and product have the same chemical composition. Therefore the transition does not involve diffusion over long distances (i.e., diffusionless).

(b) Martensitic transition are generally (though not universally) fast, compared to transitions involving diffusion; it is thought that only cooperative motions of atoms are involved and this allows the transition to proceed rapidly.

(c) The most complex and conceptually remarkable features are the reproducible crystallographic and geometric features of the transformation.

The crystallographic description of the martensite phase must deal with the following facts:

(a) The product phase is (crystallographically) coherent with the parent phase (i.e., with respect to macroscopic shape and lattice orientation).

(b) The product is a different crystalline lattice from the parent (e.g., bcc to hcp).

(c) The product phase is characterized by a fine scale inhomogeneous structure, such as slip bands or twinning. The patterns found in the product phase are characteristic of the material.

Summing up, the martensitic transformation requires a coherent distortion of the parent into a specifically oriented product having heterogeneous fine structure and a specific macroscopically unstrained interphase interface. This state of affairs can be described, phenomenologically and circumstantially, by a combination of lattice distortion, twinning or slip, and rotations.

The transformation of the body-centered cubic (bcc) structure to the hexagonal close-packed (hcp) structure is a typical martensitic transformation. The temperature-dependent bcc-hcp phase transition has been observed in many metals, (e.g., Li, Na, Zr, Ti, Hf, Tl) and alloys such as Ti-Mo. It has been suggested by Zener[3] and by Friedel[4] that the stability of the bcc phase at high temperature in these and other metals is caused by a large vibrational entropy associated with low lying shear modes. However, there has been little progress toward a detailed microscopic understanding of this phase transition. The bcc-hcp phase transition can also be induced by pressure in Ba[5], Eu and Yb.[6]

In this thesis, we study the temperature-dependent bcc-hcp phase transition in Zr and the pressure-induced bcc-hcp phase transition in Ba with use of the first-principles total energy calculations.

Several Approaches of Lattice Dynamics

(a) Harmonic approximation: Within the harmonic approximation the first goal of theory is to obtain the changes in total crystalline energy accurately to second order in the atomic displacements. The traditional method as reviewed by Born and Huang[7] or Maradudin et al.[8] is to make a formal expansion of the energy to second order (or higher) and to treat the expansion coefficients (force constants) as adjustable parameters (empirically determined). This approach has kept its utility as an interpolation and fitting scheme for experimental data with which the phonon density of states can be calculated and the lattice contribution to the specific heat determined. However, it has frequently failed as a heuristic model since for many solids with long-range forces the number of parameters required for a good fit becomes excessive and obscures the physical implications.

(b) Dielectric approach: This approach involves the determination of the valence-electron screening using linear-response theory. This method forms the basis for calculations of the simple metals[9], and is the foundation for lattice-dynamical models of covalent crystals.[10] It is formally correct for any crystal; but direct implementation of the method, which includes the precise evaluation of the dielectric matrix, has proved numerically difficult. If matrix elements are neglected (a serious approximation), the calculation is reduced to the determination of the bare susceptibility or response function, which can be easily calculated, and has been used frequently to locate nesting features of Fermi surfaces and to confirm the electronic nature of corresponding

observed phonon anomalies.[11] However, not all anomalies in the experimental phonon spectra of transition metals can be identified with structures in the susceptibility, and the magnitudes of those anomalies that have been associated with such peaks have not been determined for lack of accurate matrix elements.

(c) Empirical tight-binding method: The idea is to calculate to second order the phonon-induced changes in the total energy when it is separated into a "band-structure" term consisting of the sum of one-electron eigenvalues and a term which includes both the so-call "double-counting" energy, arising from the Hartree and exchange-correlation parts of the potential, and the ion-ion energy. To expedite their successful calculations using this method Varma and Weber considered only the band-structure term and used a set of first- and second-nearest-neighbor force constants as adjustable parameters to account for the additional short-range interactions.[12]

(d) First-principles method: Since some anomalies in phonon spectra and lattice instabilities can depend on short-range interactions, it is desirable to go beyond simple parametrization and obtain first-principles understanding of these forces. The approach to lattice dynamics which we use in this thesis involves the precise determination of the crystalline total energy as a function of the lattice displacements associated with a particular phonon. This so call "frozen phonon" method, utilizes first-principles band-structure techniques to obtain the total energy for each frozen-in position of the lattice. The phonon frequency can then be obtained from the resultant potential-energy curve. Unlike previous methods, this method

requires no experimental input to obtain the phonon frequency. Information concerning phonon anharmonicity and possible lattice instabilities can also be obtained because of the nonperturbative nature of the calculations. This is a powerful tool for studying lattice dynamics and phase transitions.

Explanation of the Thesis Format

This thesis follows the Alternate Thesis Format which permits the inclusion of papers submitted or to be submitted to scholarly journals. The research in all five sections was suggested by Dr. K.-M. Ho and Dr. B. N. Harmon, and performed under their supervision.

In Section I, a brief description for the method of calculation is given and the use of total energy calculations to study the bulk properties for Zr in the ω, bcc, hcp, fcc structures is presented. Recent neutron scattering experiments on single crystals of bcc Ba have revealed that the longitudinal branch along [100] direction is lower than the transverse branch. The calculations described in Section II are aimed at understanding the interactions responsible for this behavior. In Section III, the study of the pressure induced bcc-hcp transition in Ba is presented. We use a first principles technique to map out the energy path for the solid-solid phase transition and to study the pressure effect for the T_1 N-point phonon frequency. In Sections IV and V, we focus on the temperature-dependent bcc-hcp phase transition in Zr.

Sections II and IV were published in Physical Review B.[13,14] Sections I and III will be submitted for publication in Physical Review B. Section V and a brief description of Section III will be submitted for publication in Physical Review Letters.

SECTION I. CALCULATIONS FOR THE STATIC STRUCTURAL PROPERTIES OF Zr

Introduction

The metallic crystals formed by the Group IVA elements of the periodic table Ti, Zr, and Hf are of great interest in the study of phase transformations in the solid state. At high temperatures, they solidify to a bcc structure (β phase) but all undergo, at temperatures below T_c (1155 K, 1135 K and near 2000 K for Ti, Zr and Hf, respectively), a transformation of the martensitic variety to the hcp structure (α phase). This transformation occurs in several other metals at temperatures near the melting points. The bcc-hcp transformations in Ti and Zr are somewhat unique in that they occur at nearly one-half the respective melting temperature and involve a small but clear increase in density, i.e., $dT_c/dp < 0$.[1] There is, however, a competing transformation to the so-called ω phase which occurs both under pressure[2] in the pure metals Ti and Zr, as well as upon alloying.[3] The ω phase in materials has received extensive experimental as well as theoretical attention of physicists, materials scientists, and engineers. This is because of the complex morphology of the ω phase; its effects on physical properties such as ductility, superconductivity, etc.; the interesting kinetics of its formation; the nature of its diffuse x-ray and neutron scattering; and the mechanism of its formation from the parent bcc phase. In this paper, we shall report on first-principles total energy calculations for Zr in the hcp, bcc, fcc, and ω-phase crystal structures.

This work is part of a continuing effort to study structural phase transitions in Zr with the use of first-principles calculations. In previous work[4] we have studied the bcc to ω phase transition which involves a softening of the 2/3[1 1 1] longitudinal phonon in bcc Zr. Using 'frozen phonon' calculations, the potential energy curve as a function of atomic displacement from the bcc to ω crystal structure has been obtained. We have also performed calculations for the bcc to hcp phase transition which involves the transverse T_1 N-point mode phonon displacement and a long wavelength shear.[5] Both calculations indicate that for low temperatures the bcc phase is unstable towards the formation of the hcp and the ω-phase. We have made detailed investigations of the stabilization of the bcc phase at high temperatures by its higher entropy, the results will be described in another paper. In this paper, we focus mainly on the low temperature regime and report results for the bulk structural properties of Zr in the bcc, hcp, fcc, and ω-phase structures.

Calculations

Our calculations were performed using a first principles pseudopotential approach[6] within the local density functional formalism.[7] The only approximations entering the calculations are the standard exchange correlation potential from local density functional theory[7] (the Hedin-Lundqvist form[8] of the local exchange-correlation potential was used) and the frozen core approximation.

In the frozen core approximation, the nuclei plus the "core electrons" are considered to be rigid ions which are unresponsive to the change in their chemical environment. For Zr, although the 4p orbitals are all filled and 26 eV below the Fermi level, their wave functions are relatively extended. The slight overlap between the fully occupied 4p orbitals on neighboring atoms lead to a repulsive interaction due to the Pauli exclusion principle. On the other hand, hybridization between the 4p and the valence orbitals can lead to attraction. To find out the effect of these 'soft' core electrons on the structural properties of Zr, we have performed calculations in which the 5s, 4d, 5p, and 4p orbitals are treated as valence states in addition to the usual calculations in which the 4p electrons are treated as core electrons.

The nonlocal ionic pseudopotentials used in our calculations are generated using the norm-conserving scheme of Hamann, Schluter, and Chiang.[9] The quality of the pseudopotentials are examined by comparing the eigenvalues and excitation energies for various atomic configurations above the ground state obtained from the pseudopotentials with the corresponding all-electron values. The results for Zr are listed in Table 1. Table 1a lists the results for the case when the 4p electrons are included with the core electrons and Table 1b lists the results when both 4p and 5p electrons are treated as valence electrons. It should be noted that the results in these tables are from calculations without inclusion of spin-polarization effects and gives the $4d^2\ 5s^2$ configuration to be lower than the $4d^3\ 5s^1$ configuration. Inclusion of spin polarization effects, however, flip

the order of the two configurations. (The spin-polarization energy is 0.145 Ry for the $4d^3\ 5s^1$ configuration and 0.040 Ry for the $4d^2\ 5s^2$ configuration.) This result is in conflict with experiment - the stable configuration of the Zr atom should be $4d^2\ 5s^2$. This error comes from the local density approximation in the atomic calculations.

In order to treat systems whose electronic wave functions contain both localized atomic-like characters as well as extended plane wave-like characters, an energy independent basis set containing both plane waves and Bloch sums of localized orbitals is used to represent the electronic wave function:[6]

$$\Psi_{nk}(r) = \frac{1}{\sqrt{V}} \sum_G \alpha_n (k + G)\, e^{i(k+G)\cdot r} + \sum_{jm} \beta_{jm}(n,k)\phi_{jm}(k,r)$$

with

$$\phi_{jm}(k,r) = \frac{1}{\sqrt{N}} \sum_R e^{ik\cdot(R+\tau_j)}\, f_{jm}(r-R-\tau_j)$$

In these equations, V is the crystal volume, N is the number of atoms, and m is the label for the orbital on the j-th atom. The localized functions $f_m(r)$ are of the form

$$f_m(r) = N' r e^{-\lambda r^c} Y_{lm}(r)$$

to represent the localized part of the s, p, and d electronic wave functions. N′ is the normalization constant and c can be any positive number (for example, c=1: Slater orbitals; c=2: Gaussian orbitals, etc.).

For the calculations where the 4p states were treated as valence states, two sets of local orbitals were employed: one set to aid convergence of the 4d orbitals and another for the 4p orbitals. These numbers, c and λ, are varied to optimize the convergence of the wave function. For our plane wave energy cutoff of 10.5 Ry, we find that c=2, λ=1.13 for 4d states and c=3, λ=0.6 for 4p states give optimal convergence. For the calculations with the 4p states treated as core states, only the d orbitals are retained as local orbitals.

Sampling grids in the irreducible Brillouin zone (IBZ) contain 55 points for bcc structure, 60 points for fcc structure, and 60 points for hcp structure. For testing the sampling grids points in the IBZ, we increased the number of k-points, (for instance, 112 k-points for bcc structure, 106 k-points for hcp structure, etc.), which changes the calculated total energy by less than 0.3 mRy. Sixty k-points in the IBZ are sufficient to achieve convergence in the total energy for hcp structure, but 105 k-points in the IBZ are necessary to account for the small variation c/a in total energy for different c/a ratio at constant volume.

The ω phase has the hexagonal symmetry[10] (known as ideal ω). This structure can be described by considering the (0001) planes, which form a sequence of the type (ABAB...). The unit cell which has c/a ~0.612 contains 3 atoms, one situated in the A-plane and two in the B-plane. The space group is D_{6h} and the atomic positions are

A=(0 0 0) B=(2/3 1/3 1/2), (1/3 2/3 1/2).

Fifty seven k-points in the IBZ and the ideal c/a ratio were used to evaluate the total energy at different volumes for the ω phase.

To test the convergence of our results with respect to the basis set, we have calculated the total energies of bulk Zr with three basis sets with cutoff energies for plane waves equal to 10.5 Ry, 14.5 Ry, and 16.5 Ry. We found that increasing the plane wave cutoff from 10.5 Ry to 16.5 Ry lowers the calculated total energy by roughly 5 mRy. This is essentially a constant shift of the energy-volume curve (Table 2) which changes the calculated lattice constants and bulk moduli by less than 0.1%. Thus, in our calculations, we have used 10.5 Ry as the cutoff energy for the plane waves in our basis set.

Results and Discussion

The total energy of the crystal was calculated as a function of volume for different crystal structures. The calculated total energy versus volume curves with the 4p states were treated as valence states for bcc, fcc, hcp, and ω structures of Zr are shown in Fig. 1. The results were fitted to the universal binding curve proposed by Rose, Ferrante, and Smith[11] to obtain the cohesive energies, equilibrium volumes, and bulk moduli. No fcc phase has been observed in Zr, but its properties have been calculated by Moruzzi et al. using the KKR method.[12] Their results and the similar results we obtained are listed in Table 3. We also calculated the bulk properties where the 4p states were treated as core states. The results of our calculations, together with the comparisons with experiments, are summarized in Table

4.[2,13-17] Our calculated lattice constants and bulk moduli are in good agreement with the available experimental values. Treating the 4p states as core states leads to underestimates of the lattice constants by 2-3%. The discrepancy in the cohesive energies are bigger. It is our belief that this discrepancy is due mainly to errors of the local density approximation in treating the atom: our calculations yield the wrong ground state configuration for the atom as noted above.

Total energies were calculated for hcp Zr at different c/a ratios as well as different volumes. At the calculated equilibrium primitive cell volume (310 a.u.), a plot of energy versus c/a ratio is shown in Fig. 2. The equilibrium c/a ratio in our calculation is 1.597 which compares well with the experimental value 1.5921.[15]

The calculated band structures along symmetry directions for the bcc, hcp and ω phase Zr are plotted in Figs. 3, 4, and 5. The calculated density of states for the bcc, hcp and ω phases of Zr are plotted in Figs. 6 and 7. The Fermi energy for both the hcp and ω phase lies in a valley in the density of states while for the bcc structure it lies in a peak. Contour plots of the valence charge density for the bcc, fcc, hcp and ω structures are presented in Figs. 9, 10, 11, 12 and the corresponding geometries are shown in Fig. 8.

At a fixed temperature T and pressure P, the most stable phase of a metal is that which has the lowest Gibbs free energy

$$G = E - TS + PV,$$

where V is the volume of the metal, the quantities E and S are the total internal energy and the entropy, respectively. Because the Gibbs free energy remains constant during the bcc to hcp phase transition, one must have

$$\Delta G = \Delta E - T\Delta S + P\Delta V = 0,$$

where $\Delta X = X_{bcc} - X_{hcp}$ for any quantity X. Since the pressure P is only 1 atm and $\Delta V \sim -0.093$ cm^3/mol[18] for the bcc-hcp phase transition, the $P\Delta V$ term is negligible. Therefore

$$\Delta E(T_c) = T_c \Delta S$$

where T_c is the bcc-hcp phase transition temperature. Using the experimental $T_c\Delta S$ obtained from latent heat measurements, we get $\Delta E(T_c) = 0.041$ eV.[19] Our calculated energy difference between the bcc and hcp phases is the result corresponding to zero temperature. We can estimate from the relation

$$\Delta E(T_c) = \Delta E(0) + \int_0^{T_c} \Delta C_p dT$$

the experimental value for $\Delta E(0)$. Unfortunately, C_p for the bcc phase is not available below T_c. We give a rough estimate for the term $\int_0^{T_c} \Delta C_p dT$ as described below.

Since any C_p will be zero at T=0 K and the C_p has almost linear behavior from 300 K to T_c in hcp Zr[20], we assume that

$$C_p(T) = C_p(T_c)T/T_c$$

then

$$\Delta E(T=0\ K)_{exp} = T_c \Delta S - 1/2 \Delta C_p(T_c) T_c$$

From the experimentally measured T_c, ΔS and $\Delta C_p(T_c)$[19] we obtain $\Delta E(0)_{exp}$ ~0.058 ev/atom for Zr. A. R. Miedema and A. K. Niessen derived the enthalpy difference between bcc and hcp phases for Zr from phase diagram studies[21], their result is $\Delta E(0)$ ~0.047 ev/atom. Thus our result $\Delta E_{cal}(0)$ ~0.054 ev/atom agrees quite well with experiment.

The total energy of the ω phase was found to be slightly below that of the hcp phase. Our calculated energy difference between hcp-ω phases is -0.005 ev/atom at T=0 K. Such a small difference of energy may be within the errors of the calculations, however, we have made extensive tests of convergence and always find the ω phase to be lower (by a small amount). The energy differences between the hcp and the ω phases was obtained using the experimental c/a ratio (1.592) for the hcp structure and the ideal c/a ratio (0.612) for the ω structure. The energy of the hcp phase was lowered only by ~0.001 eV/atom at the calculated equilibrium c/a ratio (1.597). Optimizing the c/a ratio of the ω structure should also lower the energy for the ω phase. In view of our results, it is interesting to note a recent study of the hcp to ω phase transition using high resolution electron microscopy and selected area diffraction.[22] This study indicated a growth of ω phase reflection spots with the application of pressure at room temperature and also at ambient pressure when pure Zr is cooled to below 200 K. It

is concluded that the ω phase is the stable crystal phase at low temperatures. The transformation enthalpy $\Delta H^{hcp-\omega}$ deduced from this work was -553 J/ mol or -0.0057eV/atom.[22]

Conclusions

The static structural properties of the important ω phase as well as bcc, hcp and fcc structures in Zr have been studied by means of the first-principles total energy calculations. This method yielded values for the crystal lattice constant, bulk modulus, and cohesive energy in good agreement with experiment. Our results suggest that the ω phase may be the stable structure at T=0 K although the energy difference between the hcp and the ω phase are quite small, and any structural transition would proceed very slowly.

References

[1]A. Jayaraman, W. Klement, Jr., and G. C. Kennedy, Phys. Rev. 134, 644 (1963).

[2]Reference 1 and B. Olinger, J. C. Jamieson, High Temp.-High Pressures 5, 123 (1973).

[3]B. A. Hatt and J. A. Roberts, Acta Metall. 8, 575 (1960); B. S. Hickman, J. Mater. Sci. 4, 554 (1969); C. W. Dawson and S. L. Sass, Metall. Trans. 1, 2225 (1970); A. J. Perkins, P. E. Yafee, and R. F. Hehemann, Metallography 4, 303 (1971).

[4]K.-M. Ho, C.-L. Fu, B. N. Harmon, W. Weber, D. R. Hamann, Phys. Rev. Lett. 49, 673 (1982); K.-M. Ho, C.-L. Fu, and B. N. Harmon, Phys. Rev. B 29, 1575 (1984).

[5]Y. Chen, C.-L. Fu, K.-M. Ho and B. N. Harmon, Phys. Rev. B 31, 6775 (1985).

[6]S. G. Louie, K.-M. Ho, and M. L. Cohen, Phys. Rev. B 19, 1774 (1979).

[7]P. Hohenberg and W. Kohn, Phys. Rev. 136, B864 (1964); W. Kohn and L. J. Sham, Phys. Rev. 148, A1133 (1965).

[8]L. Hedin and B. I. Lundqvist, J. Phys. C 4, 2064 (1971).

[9]D. R. Hamann, M. Schluter, and C. Chiang, Phys. Rev. Lett. 43, 1494 (1979).

[10]J. M. Silcock, M. H. Davies and H. K. Hardy, Symposium on the Mechanism Phase Transformations in Metals (Institute of Metals, London, 1955).

[11]J. H. Rose, J. Ferrante, and J. R. Smith, Phys. Rev. Lett. 47, 675 (1981).

[12]V. L. Moruzzi, J. F. Janak, and A. R. Williams, Calculated Electronic Properties of Metals (Pergamon, New York, 1978).

[13]J. C. Jamieson, Science 140, 72 (1963).

[14]The experimental value of the lattice constant is for T = 862 °C, [Lattice Spacings and Structure of Metals and Alloys, edited by W. B. Pearson (Pergamon, New York, 1967), Vol. 2] while the theoretical value is strictly vaild only at T=0 K, so that the difference between the calculational and experimental values involves thermal expansion effects.

[15]J. Goldak, L. T. Lloyd, and C. S. Barrett, Phys. Rev. 144, 474 (1966).

[16]E. S. Fisher, M. H. Manghnani, and T. J. Sokolowski, J. Appl. Phys 41, 2991 (1970).

[17]L. Brewer, Lawrence Berkeley Laboratory, Report No. 3720, 1975 (unpublished).

[18]A. R. Kutsar, Fiz. Met. Metalloved 40, 786 (1975).

[19]Ralph Hultgren et al., Selected Values of the Thermodynamics Properties of the Elemants (American Society for Metals, Metals park, Ohio, 1973).

[20]C. Stassis, J. Zarestky, D. Arch, O. D. McMasters and B. N. Harmon, Phys. Rev. B 18, 2632 (1978).

[21]A. R. Miedema and A. K. Niessen, CALPHAD 7, 27 (1983).

[22]O. Botstein, A. Rabinkin and M. Talianker, Metallurgica 15, 151 (1981).

Table 1a. Eigenvalues and excitation energies of the pseudoatom for different atomic configurations of non-relativistic Zr. The 4p states are included with the core. The values in the parentheses denote the deviations from the corresponding all-electron results

Zr Configuration	Eigenvalues (Ry) 4d	5s	5p	Excitation Energy (Ry) (ΔE_{tot})
$4d^3 5s^1$	-0.1980 (0.0027)	-0.2841 (0.0014)	-0.0999 (-.0016)	0.0
$4d^2 5s^2$	-0.3068 (0.0035)	-0.3298 (0.0029)	-0.1233 (-.0015)	-0.0564 (-.0001)
$4d^4$	-0.1282 (0.0027)	-0.2545 (0.0005)	-0.0870 (-.0044)	0.1080 (0.0026)
$4d^3 5p^1$	-0.2682 (0.0035)	-0.3337 (0.0029)	-0.1416 (0.0015)	0.1877 (-.0041)
$4d^2 5s^1 5p^1$	-0.3832 (-.0018)	-0.3802 (0.0018)	-0.1640 (-.0008)	0.1548 (-.0025)
$4d^3$	-0.6245 (0.0073)	-0.6535 (0.0050)	-0.4171 (-.0001)	0.4660 (-.0030)
$4d^2 5s^1$	-0.7750 (0.0031)	-0.7328 (0.0047)	-0.4757 (0.0024)	0.4711 (-.0031)
$4d^2 5p^1$	-0.8466 (-.0010)	-0.7788 (0.0038)	-0.5177 (0.0018)	0.7799 (-.0051)

Table 1b. Similar to Table 1a. for relativistic Zr, with the 4p states treated as valence levels

Zr Configuration	Eigenvalues (Ry)				Excitation Energy (Ry)
	4p	4d	5s	5p	(ΔE_{tot})
$4d^3 5s^1$	-2.2518	-0.1887	-0.3028	-0.1005	0.0
	(0.0001)	(0.0001)	(0.0000)	(-.0014)	
$4d^2 5s^2$	-2.4015	-0.2830	-0.3424	-0.1221	-0.0886
	(-.0081)	(-.0023)	(0.0016)	(-.0024)	(0.0017)
$4d^4$	-2.1503	-0.1306	-0.2785	-0.0903	0.1324
	(0.0044)	(0.0000)	(-.0021)	(-.0015)	(0.0013)
$4d^3 5p^1$	-2.3286	-0.2592	-0.3565	-0.1442	0.2068
	(0.0072)	(0.0027)	(0.0002)	(-.0009)	(-.0012)
$4d^2 5s^1 5p^1$	-2.4818	-0.3563	-0.3954	-0.1644	0.1368
	(0.0017)	(0.0022)	(0.0030)	(-.0013)	(-.0024)

Table 2. Convergence test of the basis for Zr

Plane Waves			
Energy Cutoff (Ry)	10.5	14.5	16.5
$\Delta E^{bcc-hcp}$ (eV/atom)	0.054	0.054	0.054
$\Delta E^{hcp-\omega}$ (eV/atom)	0.0050	0.0047	0.0047

Table 3. Bulk Properties of fcc-Zr

	Lattice Constant (Å)	Bulk Modulus (Mbar)	Cohesive Energy (eV/atom)
Moruzzi et al.[12]	4.40	0.94	6.76
Present Calculation	4.49	1.0	6.95

Table 4. Comparison of the bulk properties of Zr as calculated for the bcc, hcp, and ω phase structure along with the experimental values

		calculation while the 4p states were treated as "core states"	calculation while the 4p states were treated as "valence states"	experiment
ω-phase				
Lattice Constant (Å)	a	4.93	5.04	5.04[13], 5.04[2]
	c	3.02	3.09	3.11[13], 3.14[2]
Bulk Modulus (Mbar)		1.0	1.03	1.10[2]
Cohesive Energy (eV/atom)		7.22	6.98	--
bcc-phase				
Lattice Constant (Å)		3.46	3.54	3.61[14]
Bulk Modulus (Mbar)		1.03	1.05	--
Cohesive Energy (eV/atom)		7.16	6.93	--
hcp-phase				
Lattice Constant (Å)	a	3.14	3.20	3.23[15]
	c	5.04	5.13	5.14[15]
Bulk Modulus (Mbar)		1.0	1.01	0.95[16]
Cohesive Energy (eV/atom)		7.21	6.98	6.25[17]

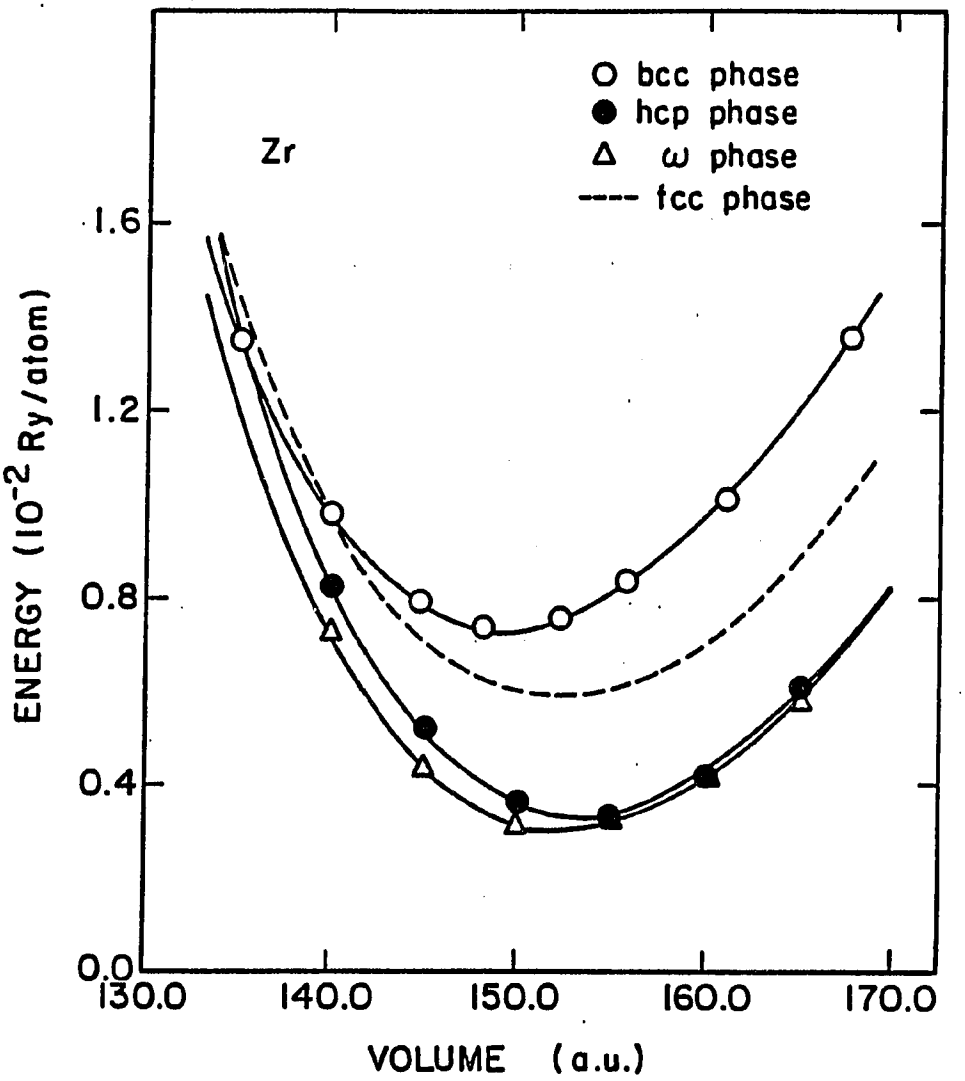

Fig. 1. The calculated total energy (per atom) for the bcc, fcc, hcp, and ω-phase of Zr as a function of atomic volume

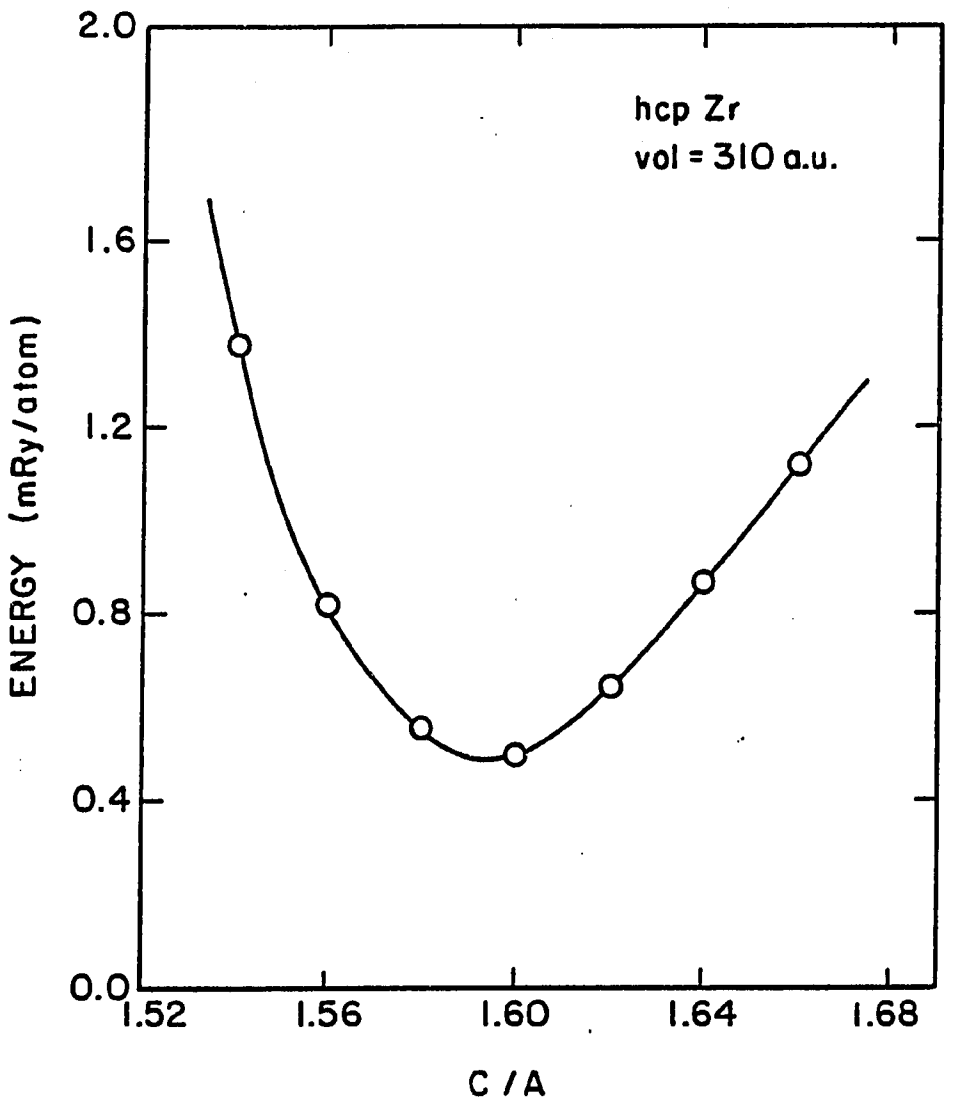

Fig. 2. The calculated total energy as a function of c/a ratio at the unit cell volume (310 a.u.). The solid line represents the fitted curve using a third order polynominal equation

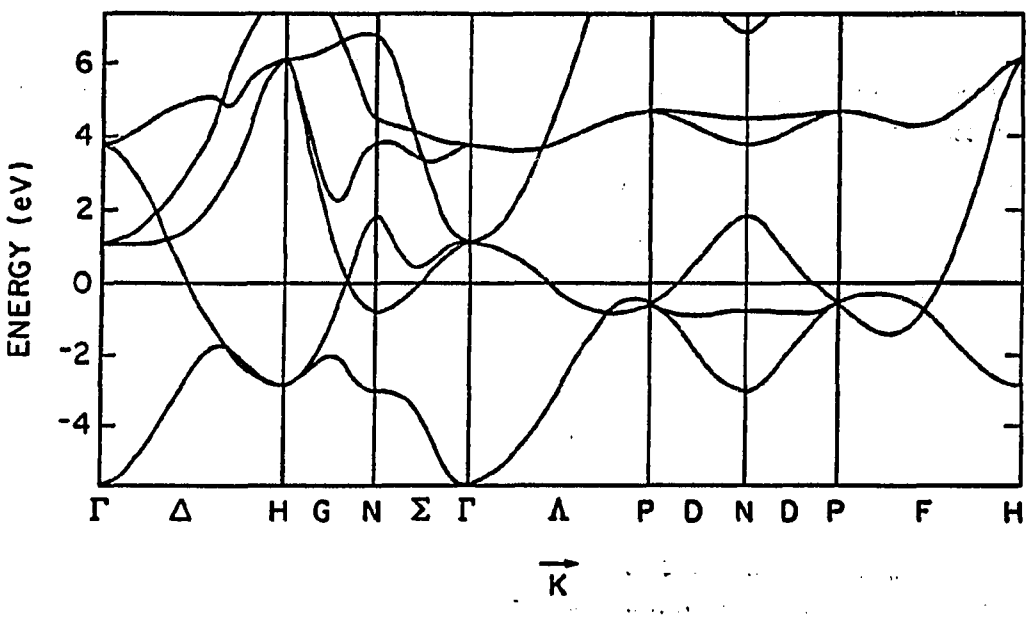

Fig. 3. Calculated electronic band structure for bcc Zr along symmetry directions

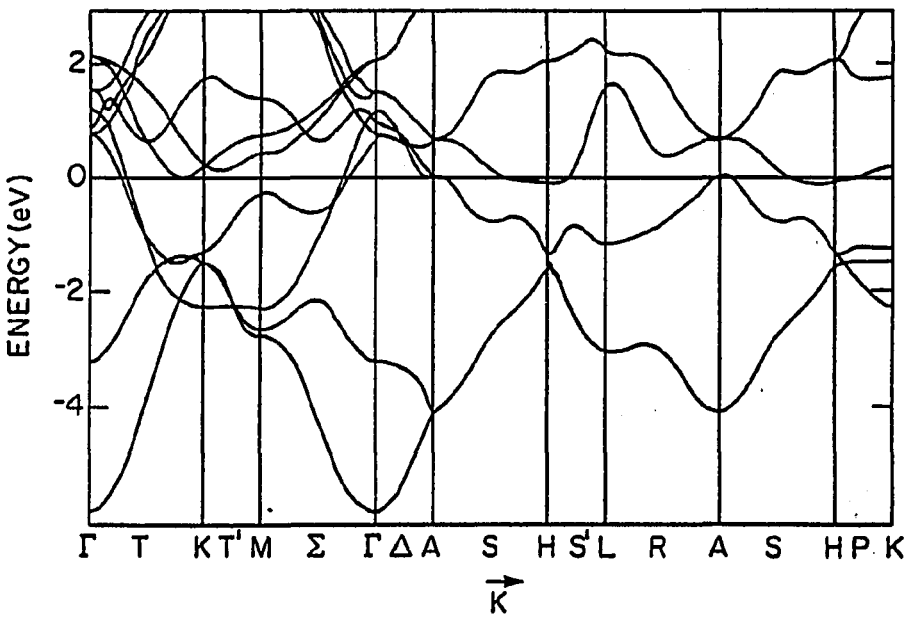

Fig. 4. Similar to Fig. 3 for the hcp phase of Zr

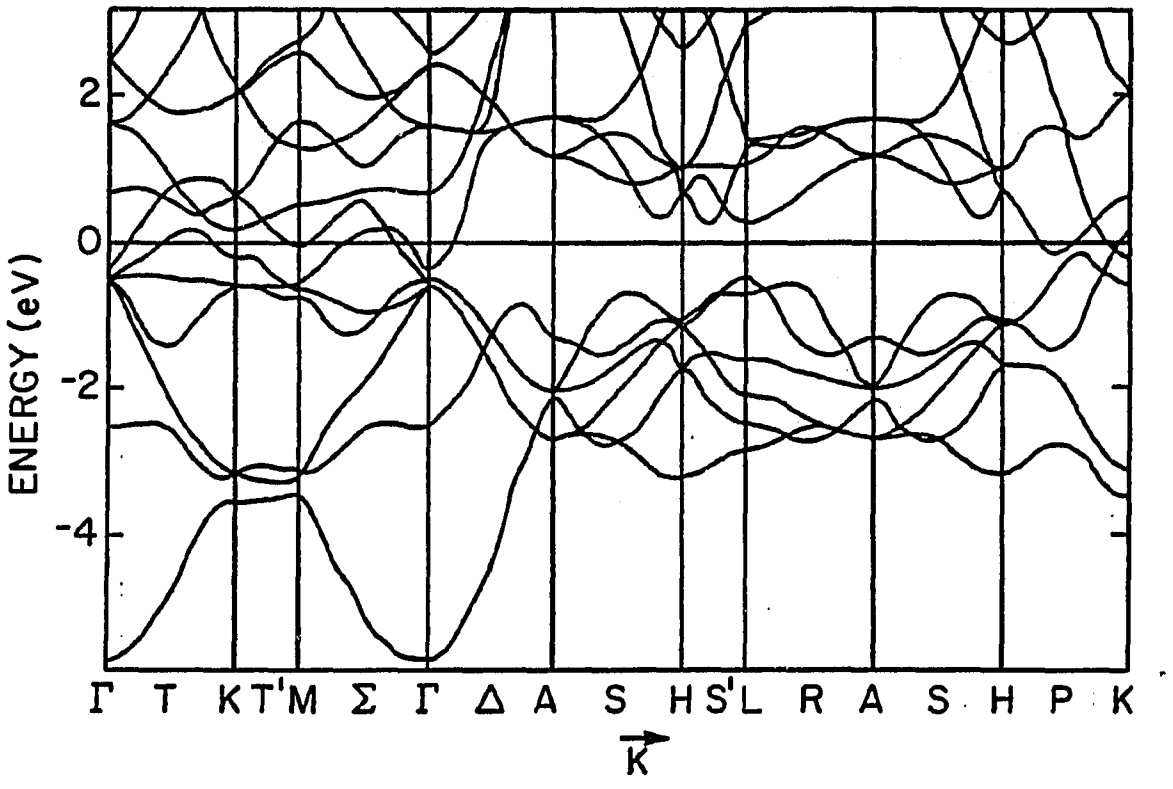

Fig. 5. Similar to Fig. 3 for the ω phase of Zr

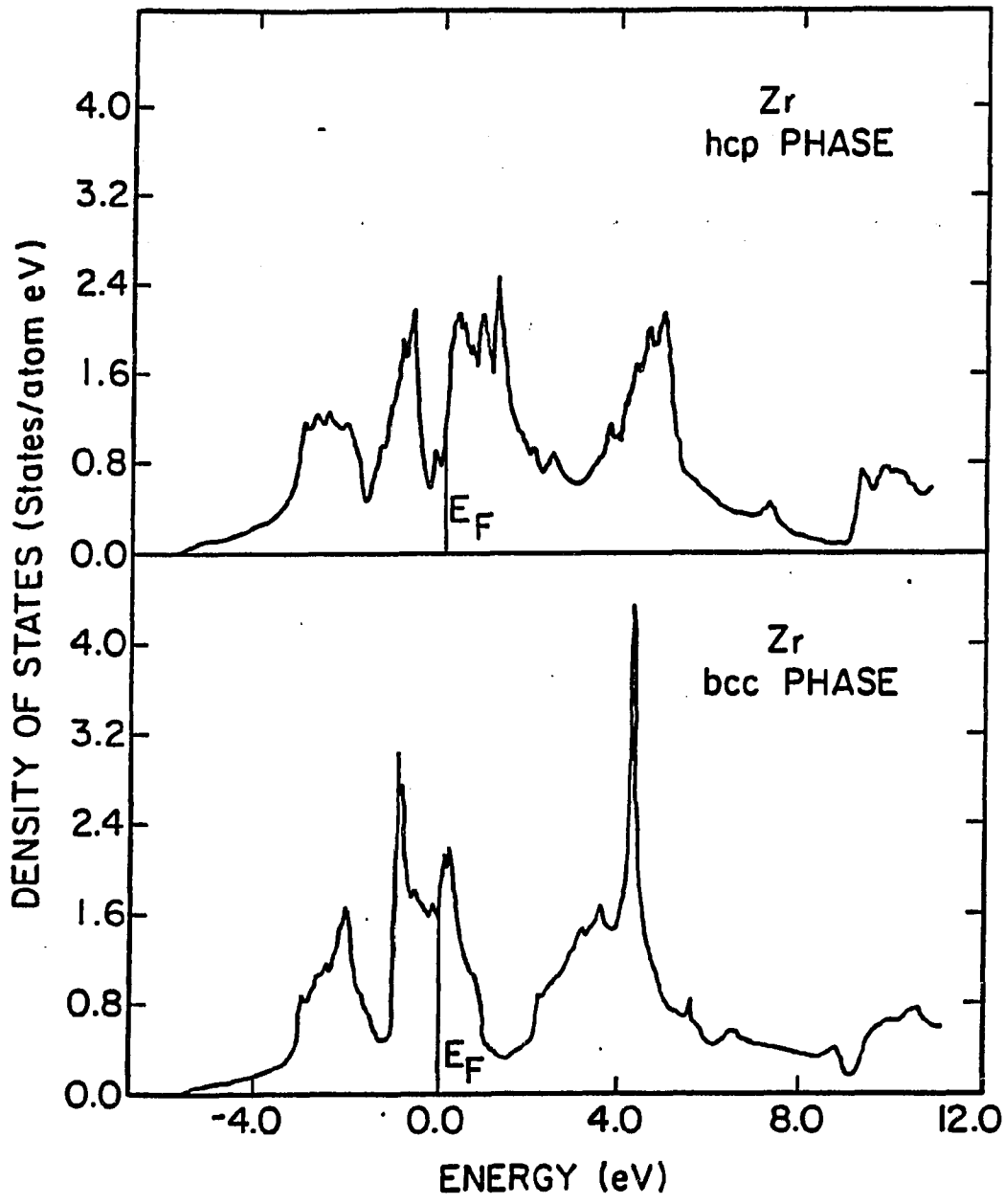

Fig. 6. The density of states for bcc and hcp Zr

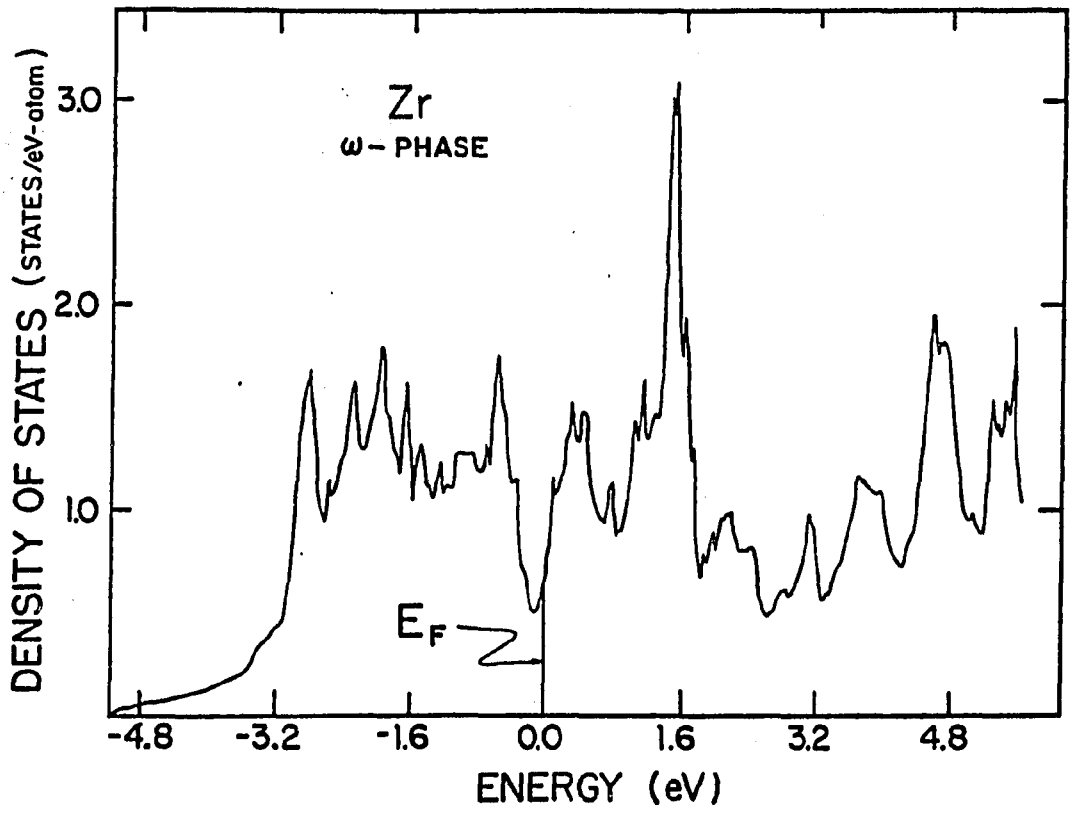

Fig. 7. The density of states for the ω phase of Zr

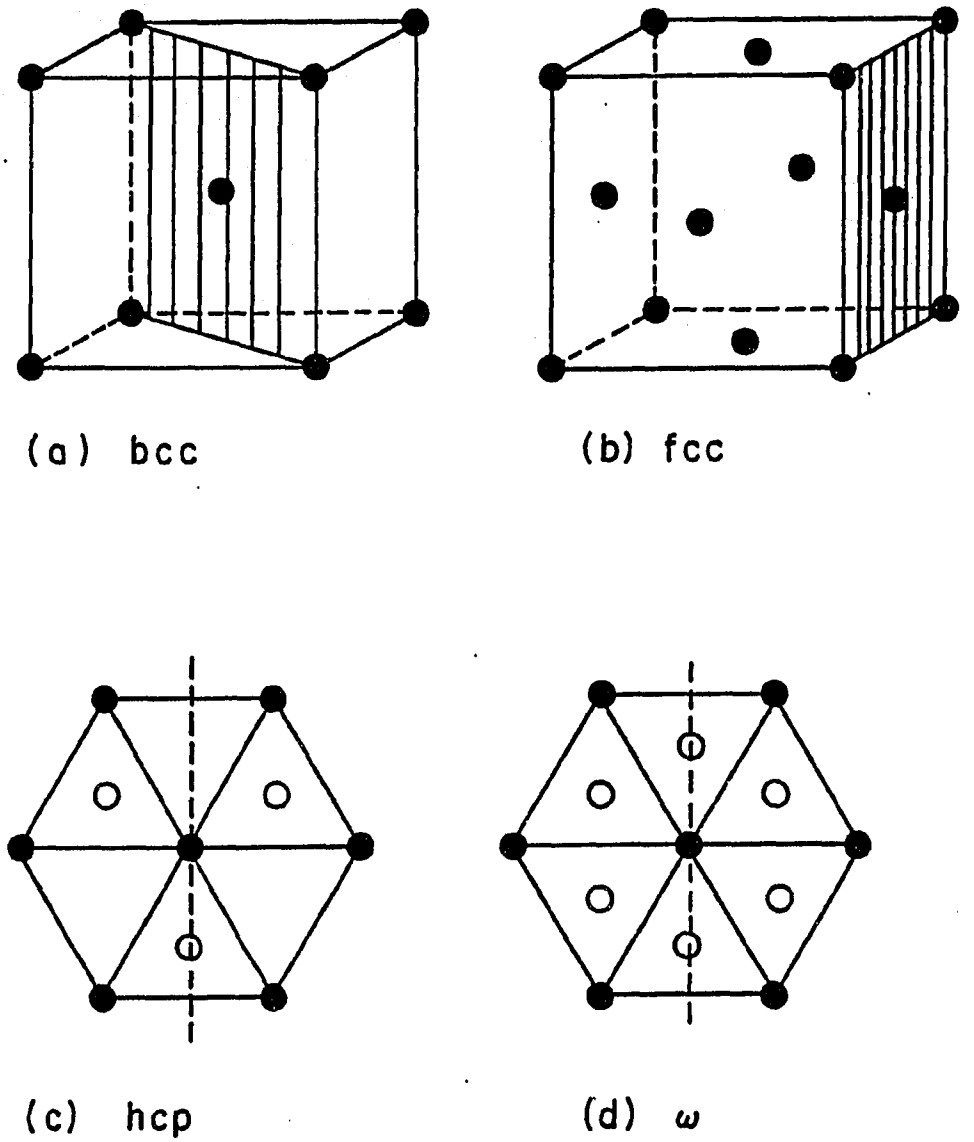

Fig. 8. Geometries for the charge plot: (a) (110) plane for the bcc phase; (b) (010) plane for the fcc structure; (c),(d) the dashed line represents the charge plot plane for the hcp and the ω phases

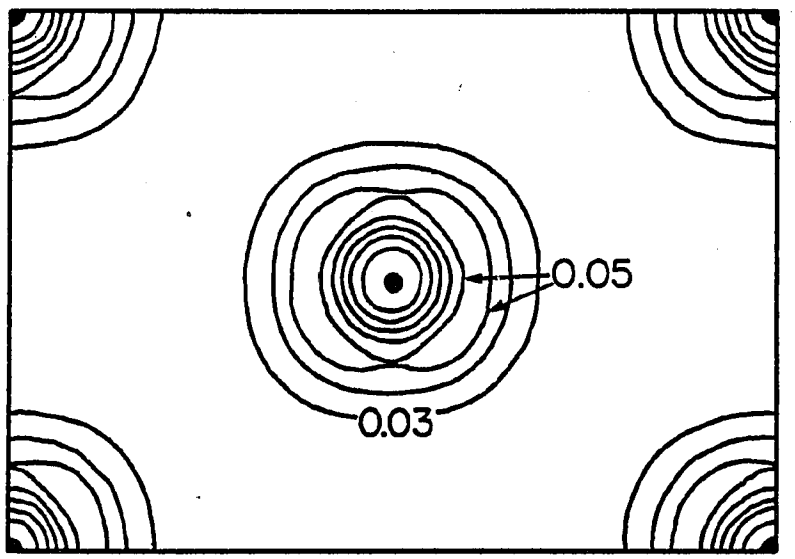

Fig. 9. The valence charge density for bcc Zr. The charge density unit is electron per unit cell volume

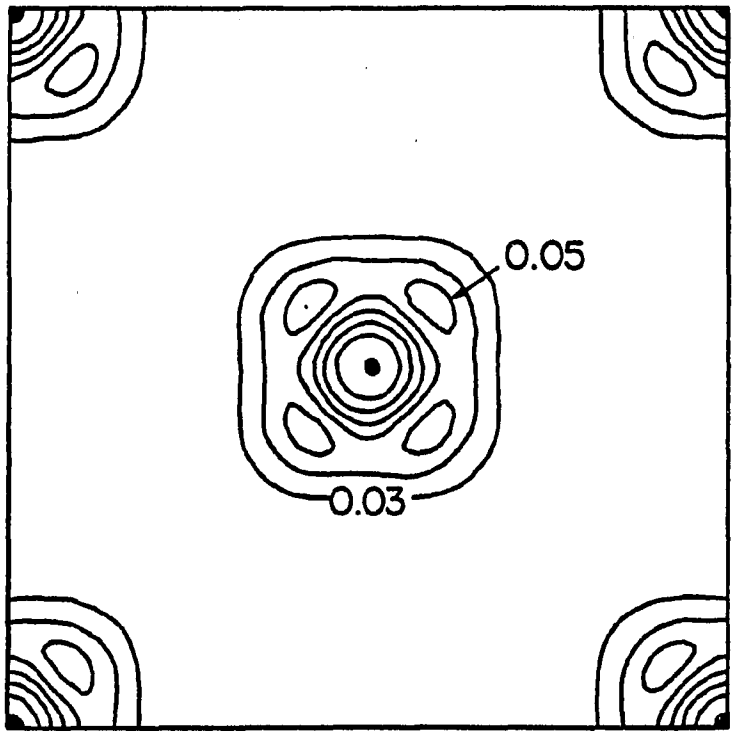

Fig. 10. Similar to Fig. 9 for fcc Zr

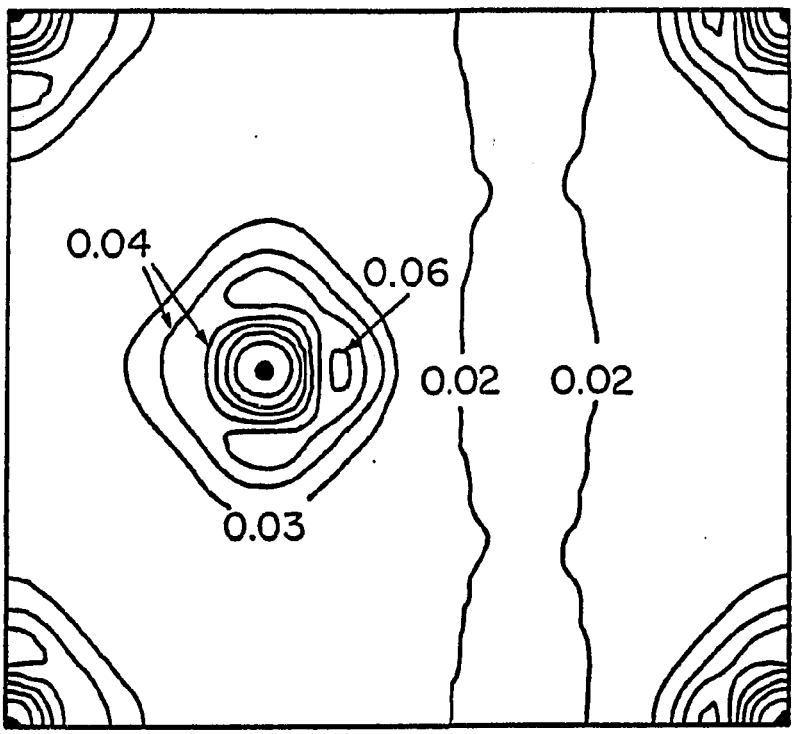

Fig. 11. Similar to Fig. 9 for hcp Zr

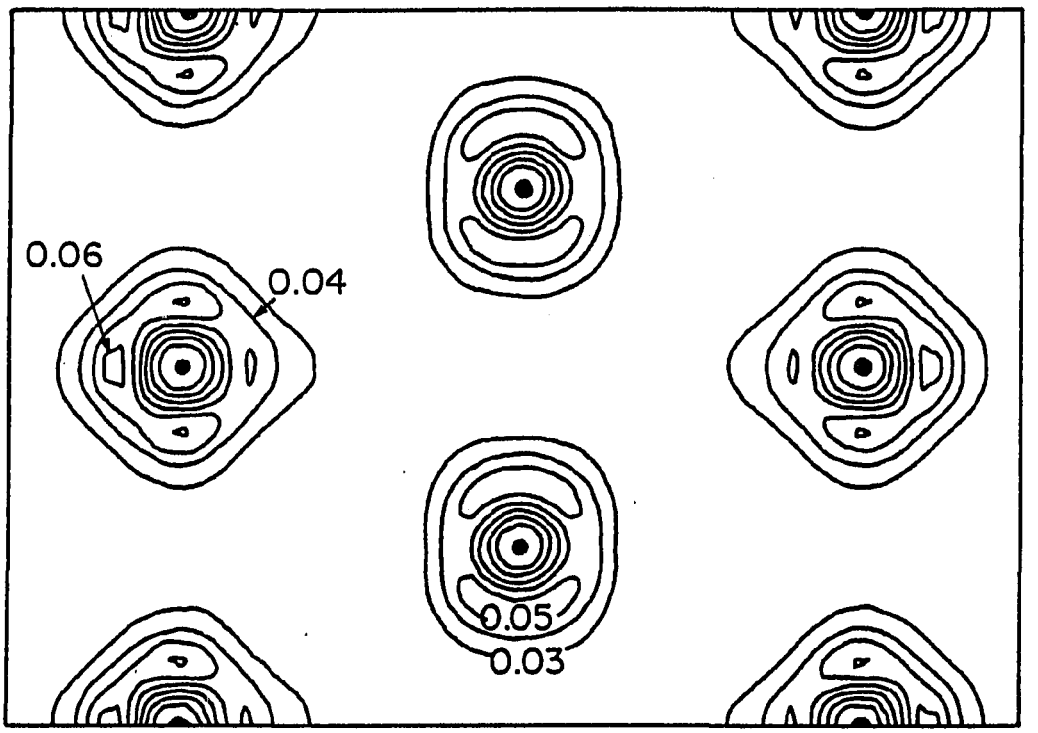

Fig. 12. Similar to Fig. 9 for the ω phase of Zr

SECTION II. ANOMALOUSLY LOW [100] LONGITUDINAL PHONON BRANCH IN Ba: THE ROLE OF THE d-BANDS

Introduction

The divalent alkaline-earth metals have long been of interest because of the different crystal structures they exhibit as a function of temperature and pressure, and also because their electronic structure is relatively simple.[1-5] The prevailing picture indicates that the free-electron like band structure, which might be expected for these metals, is modified near the Fermi level by hybridization with a broad and largely unoccupied set of d-bands. The amount of d-occupation increases with pressure and it has been correlated with the volume dependent fcc to bcc phase transition in Ca and Sr.[5] The d-occupation for Ba at ambient pressure is greater than for Ca or Sr so that the bcc phase of Ba is the stable P=0 structure.[5] Recent diamond anvil experiments on the alkaline earth metals with pressures exceeding 40 GPa have revealed further phase transitions to more complex structures.[6]

To include the effects of temperature and obtain a complete picture of the thermo-physical properties of these elements, knowledge of the lattice vibrational energies is required. Until recently, however, the difficulty in growing large single crystals has hindered the study of the lattice dynamics of these metals and only theoretical calculations of the phonon spectra have been available.[3,4,7] The situation has improved with neutron time-of-flight experiments on

polycrystalline samples of Ca and Ba which have been analyzed with Born-von Karman models to derive phonon dispersion curves.[8,9] In addition, large single crystals of fcc Ca, bcc Ba, and the high temperature bcc-phase of Sr were grown for the first time, and the phonon dispersion were curves measured directly using inelastic neutron scattering techniques.[10-12] The phonon dispersion curves of Ba obtained by these direct measurements revealed that the [100] longitudinal branch is lower than the transverse branch.[11] This is quite anomalous and does not occur in the measured dispersion curves of bcc Sr.[12] Also the previous theoretical calculations for the phonon spectra of Ba have not predicted this unusual feature.[3,4,7] The calculations described in this paper were aimed at understanding the interactions responsible for this behavior. By performing calculations both with and without the d-states, we find that the [100] longitudinal branch is lowered because of strong interactions with the electronic states having d-like character.

Procedures and Results

Bulk Properties

Before investigating the phonons along the [100] direction, the methods and programs for Ba were tested by first evaluating some of the bulk equilibrium properties. The total energy calculations were performed within the local density functional formalism,[13] using the Hedin-Lundqvist form[14] for approximating the electronic exchange and correlation energy. The electronic structure was calculated using a

self-consistent, first-principles pseudopotential technique, which should not be confused with the empirical, perturbative methods used previously for Ba.[2-4,7] The nonlocal ionic pseudopotential was generated from relativistic first-principles atomic calculations (without spin-orbit coupling[15]) according to the norm-conserving scheme of Hamann, Schluter and Chiang.[16] The method has been used successfully for a wide variety of materials and the reader is referred to our previous work on transition metals for a more complete list of references.[17] For Ba the calculation of the bulk properties was carried out for both the fcc- and bcc-phases. The total energy of the crystal was determined at eight different volumes, and these values were used for a non-linear least squares fit to obtain the equation of state. The functional form of the equation of state was the universal bonding curve,[18] although the results near the equilibrium volume are not sensitive to the analytical form chosen. The curves are shown in Fig. 1. For the bcc lattice, convergence was achieved by using 112 k-points in the 1/48th of the Brillouin zone and a plane wave cut-off energy of 8.5 Ry. For the fcc lattice, a similar convergence (better than 0.0002Ry on the total energy) was obtained using 60 k-points in the irreducible zone and the same cut-off energy. The results of the calculations are given in Table 1[19-21] along with the experimental values of the lattice constant, bulk modulus, and cohesive energy. The agreement between theoretical and experimental values is quite good. The 4% discrepancy with the lattice constant is larger than for more strongly bonded crystals, partly because the total energy of the crystal changes very little as a function of volume as evidenced by the

small bulk modulus.[22] This discrepancy is consistent with results found by other workers for Ca and Sr,[23] and might be attributed to errors due to the local density approximation.

For comparison with previous calculations we show the energy bands along the high symmetry directions in Fig. 2. These bands were obtained using the experimental, low temperature value of the lattice constant (a=5.000Å). The corresponding electronic density of states is shown in Fig. 3. The density of states at the Fermi level, $N(E_F)$, is 1.07 states/eV-atom. The experimental value of the electronic specific heat ($\gamma = 2.7 \pm 0.5$ mJ/mole K)[24] implies a density of states of 1.15 ± 0.2 states/eV-atom which indicates a small electron-phonon enhancement. A previous non-selfconsistent RAPW calculation by Johansen resulted in a slightly higher $N(E_F)$ of 1.35 states/eV-atom, and a band structure very similar to ours.[25] Unlike Johansen's bands we do not have any 4f states appearing at about 0.3 Ry above E_F, since we did not include a separate l=3 part to our non-local pseudopotential. Calculations by Duthie and Pettifor,[26] and by Herbst[27] show that the 4f states remain well above E_F even at high pressures and should not affect any of the properties we deal with in this paper.

To better isolate the contribution made by the d-states of Ba, we have performed calculations with the l=2 part of the pseudopotential shifted -- which has the effect of raising the energy of the d states. The density of states for the bands with the d bands removed in this fashion is also shown in Fig. 3 and the comparison with the normal density of states gives dramatic evidence for the transition metal-like band structure of Ba. The energy bands with the d states shifted is

shown in Fig. 4. Calculations of the total energy vs volume for Ba using this potential to shift the d bands well above E_F resulted in the equilibrium volume expanding by ~ 60% and the cohesive energy decreasing by 1.2 eV. This again emphasizes the important role played by the d-bands in determining the physical properties of Ba.

Phonon Anomaly

The measured phonon dispersion curves along the [100] direction are shown in Fig. 5.[11] At reduced wave vectors larger than 0.1, where measurements could be made, the longitudinal branch is lower than the transverse, with the largest deviations (~0.3THz) occurring in the region halfway to the zone boundary. To understand this anomalous behavior we performed frozen phonon calculations for reduced wave vectors of 0.5 and 1.0 (the H point). The procedure requires the accurate calculation of the total energy of the crystal as a function of the atomic displacement. The atoms are displaced in directions corresponding to the polarization vector of the phonon being studied, and at each fixed position a fully self-consistent band structure calculation is performed. The total energy determined at several small values of the displacement is fit with a quadratic function, $1/2\ m\omega^2\delta^2$, from which the phonon energy, $\hbar\omega$, is determined.[28] Table 2 lists the phonon frequencies obtained by this method. Halfway to the zone boundary the longitudinal branch is found to be lower than the transverse by ~0.2THz in good agreement with experiment. The theoretical phonon frequencies are shown in Fig. 5 as squares. Also listed in Table 2 are the frequencies of the phonons halfway to the

zone boundary obtained by exactly the same method, but with the l=2 part of the pseudopotential shifted as discussed above so that the d-bands were no longer in the region of the Fermi level. The effect of removing the d-bands is to raise the transverse frequency by 0.44THz and the longitudinal frequency by 1.17THz. Thus, without the screening from d-like states, the branches are ordered in the normal position and shifted to higher frequencies. This is consistent with the situation found in Sr where the d-bands are located higher above E_F and the frequencies along the [100] direction are in the normal order.

Conclusions

Although there has been growing evidence that the d bands play an important role in determining the structure and physical properties of Ba, it is not generally appreciated how much of a "transition-metal" Ba actually is. The comparison of the density of states of Ba and of a hypothetical Ba with d bands removed (Fig. 3) gives a clear picture of the amount of d-like character extending well below the Fermi-level. We have shown by using the frozen phonon method that the d-states are responsible for the anomalously low [100] longitudinal phonon branch in Ba. The previous difficulty in finding this phonon anomaly by other methods is probably a result of the limited applicability of those methods when extended to transition metals.

References

[1] M. F. Manning and H. M. Krutter, Phys. Rev. 51,761 (1937).

[2] B. Vasvari, A. O. E. Animalu, V. Heine, Phys. Rev. 154, 535 (1967).

[3] A. O. E. Animalu, Phys. Rev. 161, 445 (1967).

[4] J. A. Moriarty, Phys. Rev. B 6, 4445(1972); 8, 1338 (1973).

[5] H. L. Skriver, Phys. Rev. Lett. 49, 1768 (1982); Phys. Rev. B 31, 1909 (1985).

[6] H. Olijnyk and W. B. Holtzapfel, Phys. Lett. 100A, 191 (1984).

[7] K. S. Sharma, Phys. Status Solidi (b) 108, K101 (1981).

[8] U. Buchenau, H. R. Schober, and R. Wagner, J. Phys. (Paris) Colloq. 42, C6-395 (1981).

[9] U. Buchenau, M. Heiroth, H. R. Schober, J. Evers, and G. Oehlinger, Phys. Rev. B 30, 3502 (1984).

[10] C. Stassis, J. Zaretsky, D. K. Misemer, H. L. Skriver, B. N. Harmon, and R. M. Nicklow, Phys. Rev. B 27, 3303 (1983).

[11] J. Mizuki, Y. Chen, K.-M. Ho, C. Stassis, Phys. Rev. B 32, 666 (1985).

[12] J. Mizuki and C. Stassis, Phys. Rev. B 32, 8372 (1985).

[13] P. Hoberberg, W. Kohn, Phys. Rev. 136, B864 (1964); W. Kohn and L. J. Sham, Phys. Rev. 140, A1133 (1965).

[14] L. Hedin and B. I. Lundqvist, J. Phys. C 4 2064 (1971).

[15] D. D. Koelling and B. N. Harmon, J. Phys. C 10, 3107 (1977).

[16] D. R. Hamann, M. Schluter, and C. Chiang, Phys. Rev. Lett. 43, 1494 (1979).

[17] K.-M. Ho, C.L. Fu, and B.N. Harmon, Phys. Rev. B 29, 1575 (1984).

[18]J. H. Rose, J. Ferrante, and J. R. Smith, Phys. Rev. Lett. 47, 675 (1981).

[19]W. B. Pearson, A Handbook of Lattice Spacings and Structures of Metals and Alloys (Pergamon, New York, 1967), Vol. 2.

[20]K. Gschneidner, Jr., Solid State Physics 16, 308 (1964).

[21]L. Brewer, Lawrence Berkeley Laboratory Report, No. 3720, 1975 (unpublished).

[22]The bulk modulus obtained by using the elastic constants determined from the single crystal neutron scattering experiments (Ref. 11) is a factor of four smaller than the value given in Table 1. This, we believe, indicates the longitudinal branch near q=0, where the neutron scattering experiments were unable to measure, is probably higher than the transverse branch.

[23]J. P. Jan and H. L. Skriver, J. Phys. F 11, 805 (1981).

[24]L. M. Roberts, Proc. Phys. Soc. B 70, 738 (1957).

[25]G. Johansen, Solid State Commun. 7, 731 (1969).

[26]J. C. Duthie, and D. G. Pettifor, Solid State Commun. 27, 613 (1978).

[27]J. F. Herbst, Phys. Rev. B 22, 1600 (1980).

[28]A more complete description of the frozen phonon method is given in Ref. 17. The basic assumption on which the method is based is that the electronic motion is so much faster than the ionic motion that at any instant the electrons are in the self-consistent ground state defined by the instantaneous configuration of the ions. M. Born and R. Oppenheimer, Ann. Phys. (Leipzig) 84, 457 (1927).

Table 1. A comparison of the bulk properties of Ba as calculated for the fcc and bcc structure along with the experimental values

	Lattice Constant (Å)	Bulk Modulus (Mb)	Cohesive Energy (eV)
bcc-Ba:			
Calculation	4.80	0.11	2.01
Experiment	5.00[19]	0.105[20]	1.90[21]
fcc-Ba:			
Calculation	6.02	0.103	2.00

Table 2. A comparison of the experimental and theoretical phonon frequencies of bcc-Ba at q = (0,0,1/2) and the H-point

	q = (0,0,1/2)		q = (0,0,1)
	L-phonon (THz)	T-phonon (THz)	H-point phonon (THz)
Calculation	1.38	1.55	2.20
Calculation with d-bands removed	2.55	1.99	--
Experiment[a]	1.22 ± 0.12	1.52 ± 0.04	2.15 ± 0.07

[a]Reference 11.

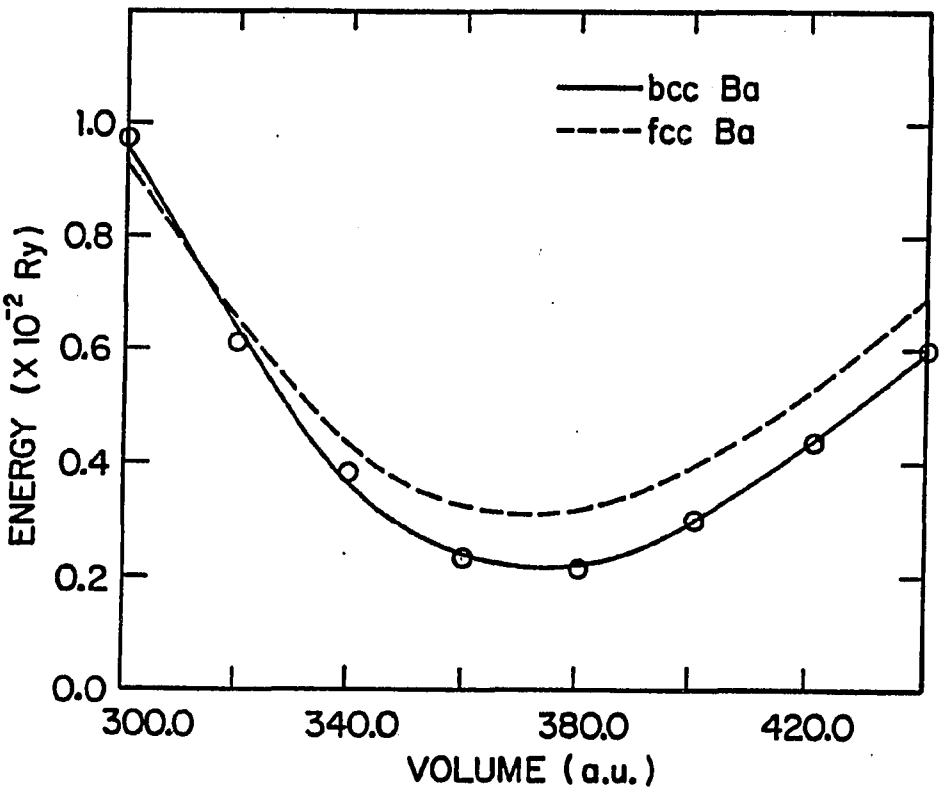

Fig. 1. The total energy (per atom) versus volume for bcc and fcc Ba. The minimum for bcc Ba corresponds to a lattice constant of 4.80 Å

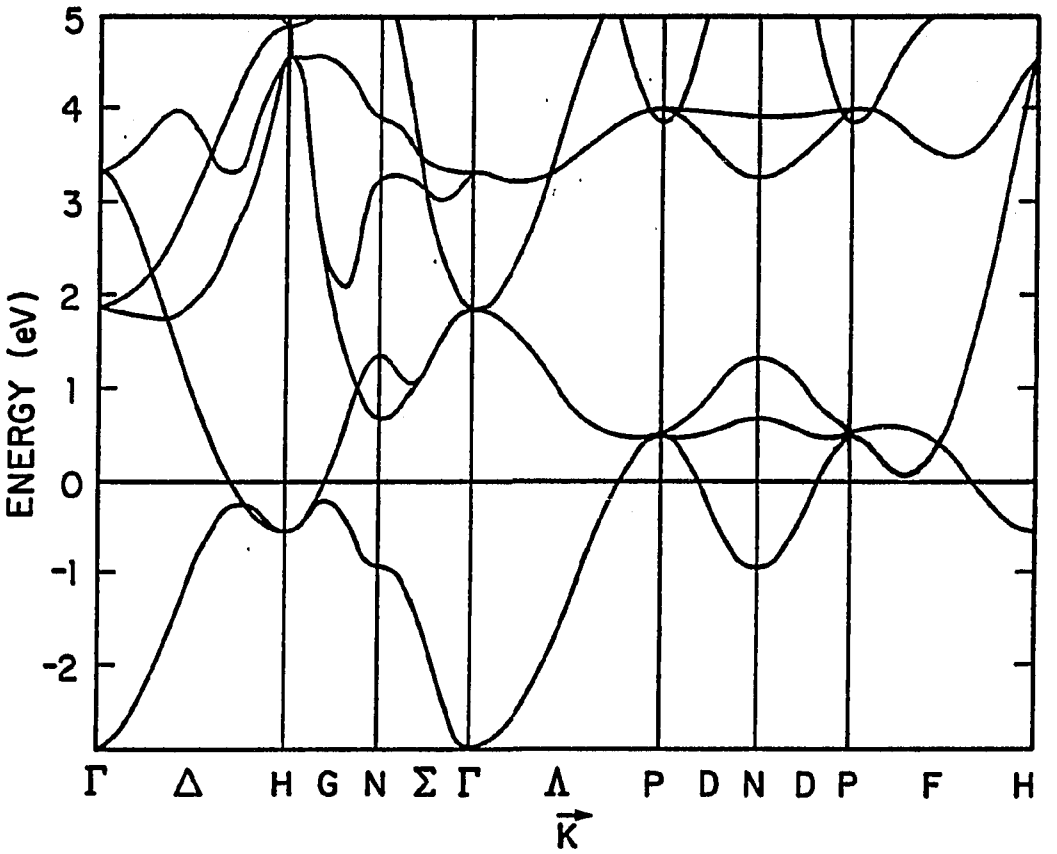

Fig. 2. The energy bands of bcc Ba calculated at the experimental volume using a first principles pseudopotential method

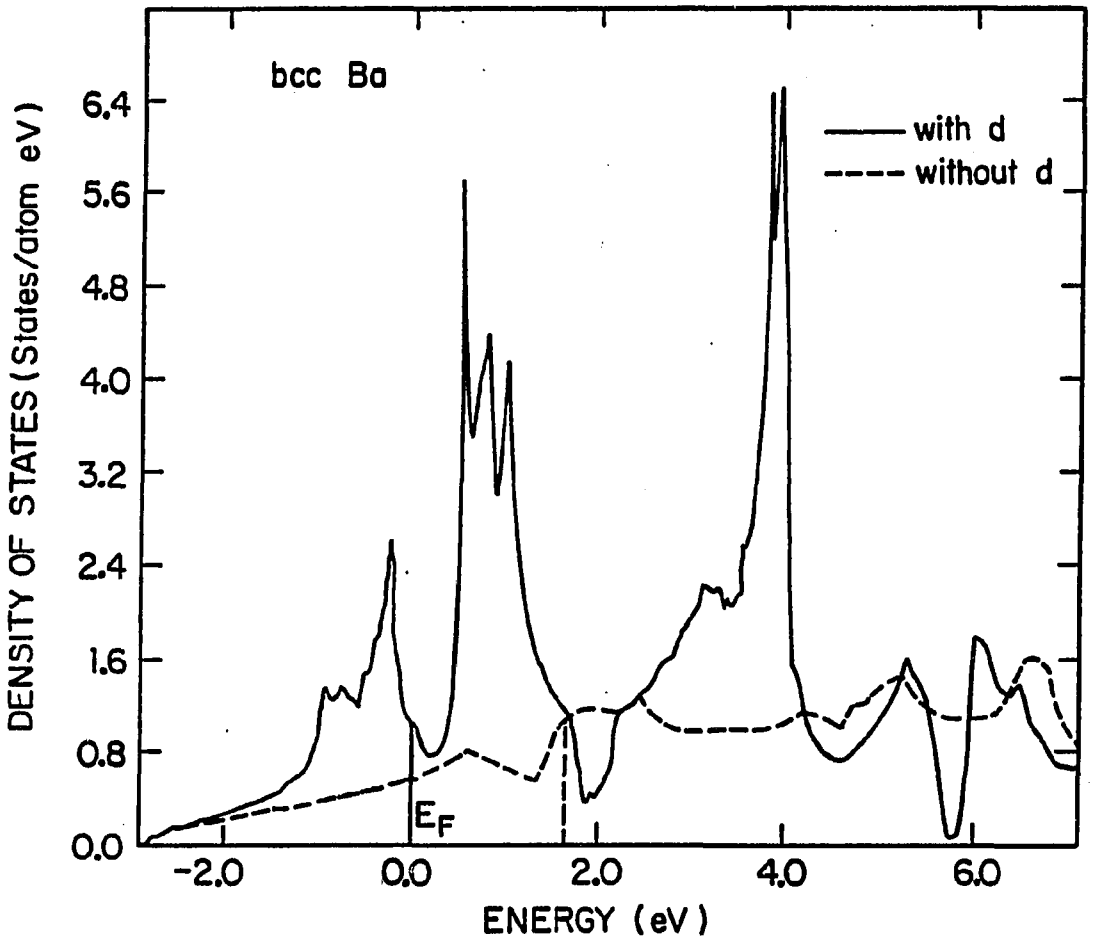

Fig. 3. The density of states for bcc Ba. The dashed curve is the result from calculations with the d bands shifted to an energy range above the scale shown. The vertical dashed line is the Fermi energy for the calculation with the d bands shifted

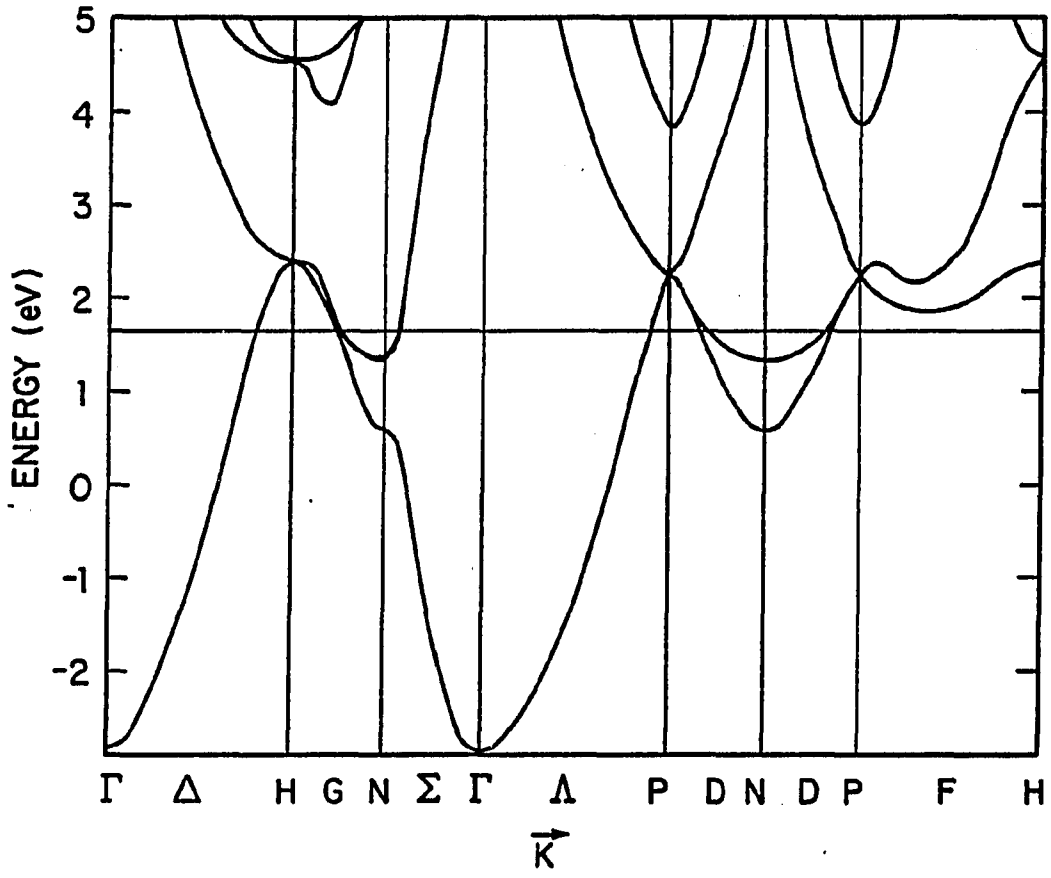

Fig. 4. The energy bands for bcc Ba with the d bands removed by shifting them to higher energies. The corresponding density of states is the dashed curve in Fig. 3

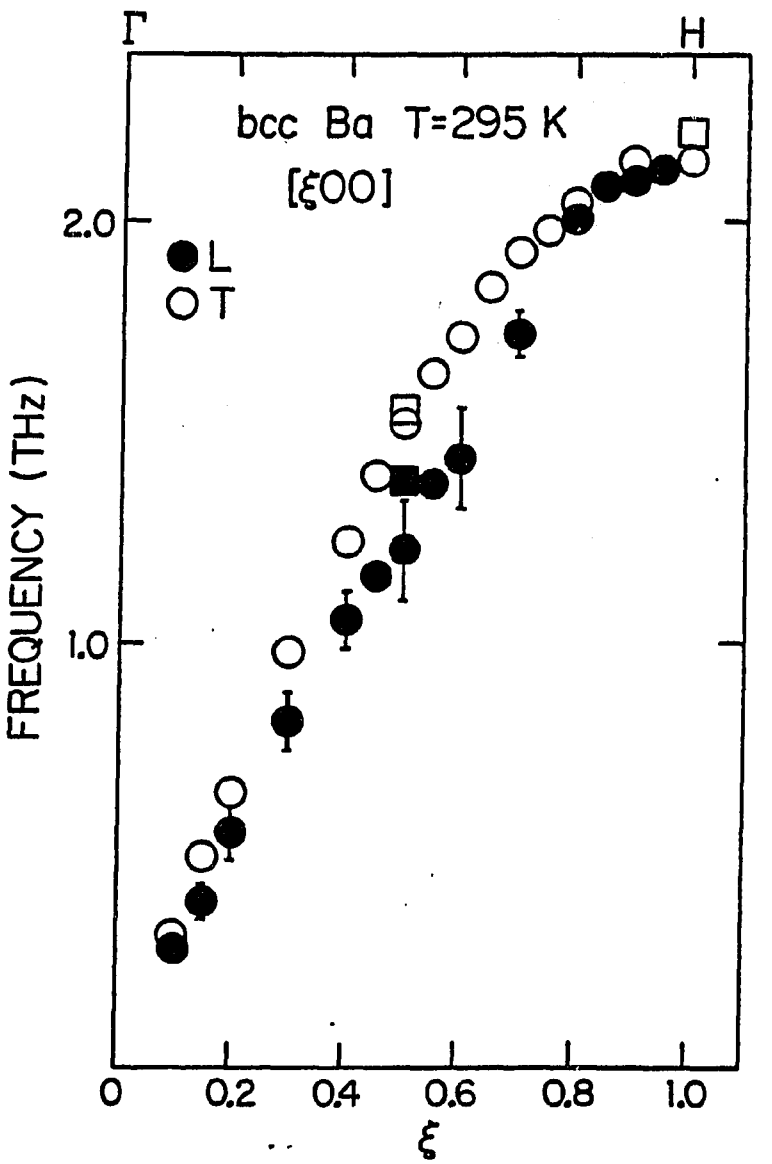

Fig. 5. The experimental phonon frequencies from Ref. 11. The corresponding theoretical phonon frequencies obtained by the frozen phonon method are shown as squares

SECTION III. FIRST-PRINCIPLES STUDY OF THE PRESSURE INDUCED bcc-hcp TRANSITION IN Ba

Introduction

The subject of phase transitions in solids is a well established discipline with most of our understanding based on phenomenological models.[1,2] Recently, however, precise first principles calculations of material dependent features of phase transitions and other physical properties have become feasible. This progress has been achieved through the development of accurate methods to calculate the total energy difference associated with atomic displacements in solids. These techniques have been used with great success in first principles studies of lattice vibrations in various crystals via 'frozen phonon' calculations. In addition to giving an accurate description of the harmonic forces, these methods also include the anharmonic contributions and thus are inherently more powerful than tranditional phonon methods in studying structural phase transition where the phonon mode goes soft. Martensitic phase transitions are ideally suited for studies using 'frozen phonon' methods. The parent and resultant crystal orientations are closely correlated limiting the number of paths and hence configurations needed to be studied in the calculations.

The transformation of the body-centered cubic (bcc) structure to the hexagonal close-packed (hcp) structure is a typical martensitic transformation. The temperature-dependent bcc-hcp phase transition has

been observed in many metals, (e.g., Li, Na, Zr, Ti, Hf, Tl) and alloys such as Ti-Mo. The pressure-induced bcc-hcp phase transition has been observed in Ba, Eu and Yb.[3,4] Ba transforms to the hcp structure at room temperature at a pressure of 55 kbar.[4] The transformation pressure decreases as the temperature is lowered.[5] This is a first order phase transition with a volume change of ~1.9% or 0.72 cm^3/mole.[6]

In this paper we focus on the pressure induced bcc to hcp phase transition in barium. Using first-principles total energy calculations we have obtained the complete energy surface from the bcc to the hcp structure at fixed volumes for several lattice volumes on both sides of the phase transition. Analysis of these energy surface provides interatomic potentials which can be used in future molecular dynamics simulations to study the kinetics of the phase transition. Previous theoretical work includes the first principles calculation by H. L. Skriver which predicted the bcc to hcp transition in Ba at ~100 kbar[7], however, he did not study the transition path or the important role played by the T_1 N-point phonon in the phase transformation. A much earlier study of the phase transition in Ba was made by Animalu, however he was limited by the use of an empirical approach.[8]

Below we first orient the reader by providing a geometrical description of the transition. The calculations are then described and the results given in terms of contour plots for the transition energy surface. The discussions and summary are given in the last section.

Transition Coordinates

The crystallographic relations in the bcc-hcp martensitic phase transition were established in 1934 by Burgers[9]:

$$(110)_{bcc}//(001)_{hcp},\ [111]_{bcc}//[110]_{hcp}$$

These relations can be achieved by a transformation scheme which involves atomic displacements corresponding to the zone boundary [110] T_1 phonon mode (Fig. 1 (a)) and a subsequent shearing of lattice: A displacement of $\delta = \sqrt{2}/12a$ creates a nearly hexagonal geometry (the dashed lines in Fig. 1 (b)), a shear is then required to change the angle θ from 109.47° to 120.0°, and establish the hcp structure (Fig. 1 (c)). For bcc crystals which exhibit a transition to the hcp phase the [110] T_1 branch is indeed low in energy, indicating a weak restoring force for the displacement required in the transition.[10] For the actual transition path one expects motion corresponding to the shear and the [110] T_1 displacements to occur simultaneously. We calculate the actual path as a function of both these coordinates.

Calculations and Results

Our calculations were performed using the first-principles pseudopotential approach within the local density-functional formalism.[11] The only approximations made in these calculations are the local density approximation for the exchange-correlation energy

(the Hedin-Lundqvist form[12] was used), the frozen core approximation, and the Born-Oppenheimer approximation.[13] The nonlocal ionic pseudopotential was generated according to the norm-conserving scheme of Hamann, Schluter and Chiang.[14] The quality of the pseudopotentials are examined by comparing the eigenvalues and excitation energies for various atomic configurations with the corresponding all-electron values. The results for Ba are listed in Table 1. This method has been successfully applied in the calculation of structural and dynamical properties for a wide variety of materials.[15,16] In our calculations, the 5p electrons are treated as valence electrons and the wave functions in the solid are expanded in terms of a mixed basis[17] of local orbitals plus plane waves:

$$\Psi_{nk} = \frac{1}{\sqrt{V}} \sum_{G} \alpha_n (k + G)\, e^{i(k+G)\cdot r} + \sum_{jm} \beta_{jm}(n,k)\, \phi_{jm}(k,r)$$

with

$$\phi_{jm}(k,r) = \frac{1}{\sqrt{N}} \sum_{R} e^{ik\cdot(R+\tau_j)}\, f_{jm}(r-R-\tau_j)$$

The localized functions $f_m(r)$ are here chosen of the form

$$f_m(r) = N' r e^{-\lambda r^c} Y_{1m}(r)$$

to represent the localized part of the 5p electronic wave functions. N' is the normalization constant. The numbers c and λ are varied to optimize the convergence of the wave functions. For our plane wave

energy cutoff of 8.5 Ry we find that c=3, λ=0.19 for 5p states give optimal convergence. We have found that the 5p states make significant contribution to the physical properties, while the contribution of the 5s states is negligible in our calculations. Treating the 5p states as frozen core states, we used plane waves up to the energy cutoff of 8.5 Ry to represent the 6s, 6p and 5d states, the calculated equilibrium lattice constant is ~6% smaller than that of treating the 5p states as valence states. In a previous study the bulk properties of bcc Ba were evaluated and an anomaly in the [100] phonon dispersion curves explained.[18] A summary of the bulk properties and the selected phonon frequencies of bcc Ba are listed in Table 2.[19-24] The energy bands along the high symmetry directions for bcc Ba at $V=V_{exp}$ and under pressure ($V=0.71V_{exp}$) are plotted in Figs. 2 and 3, the corresponding densities of states are presented in Fig. 4. These figures indicate that the d-like character of the occupied electronic states increases with pressure as was first stressed by Vasvari et al.[25]

The frozen phonon calculations were made to evaluate the frequency of the zone boundary [110] T_1 mode at the N-point. The atoms are displaced in directions corresponding to the polarization vector of the phonon, and at each fixed position a fully self-consistent band structure calculation is performed and the total crystalline energy is evaluated.[26] With distortions of the crystal corresponding to the T_1 N-point phonon mode displacements, the original cubic symmetry of the bcc lattice is reduced to D_{2h} (8 group operations), and the real-space unit cell is doubled. Convergence was achieved by using 176 k-points in the 1/8th of the irreducible Brillouin zone. The total energy

versus atomic displacement curves have been calculated for four different atomic volumes. The results are ploted in Fig. 5. For small displacements, the quadratic part of the curves may be used to obtain (via $\Delta E=1/2m\omega^2\delta^2$) the harmonic frequencies. The $V=V_{exp}$ curve yields a frequency of 0.7 THz in excellent agreement with experimental value of 0.75 ± 0.04 THz.[24] The frequency decreases with increacing pressure and goes to zero at a reduced volume of $0.73V_{exp}$ (corresponding to a pressure of 31 kbar[27]). However, before the T_1 N-point phonon becomes soft, the energy of the hcp phase is already lower than the bcc phase as described below.

To obtain the bcc-hcp phase transition path, we calculated the total energy of the crystal as a function of the phonon displacement and the angle of the shear motion for three different atomic volumes. With the atomic displacements corresponding to the T_1 N-point phonon mode and the shear motion, the symmetry of these intermediate structures is D_{2h} which is the same as that of the T_1 N-point phonon. We used the same 176 k-point for the sampling grids in the IBZ. At each volume, the total energy was calculated for nine different angles and thirteen different displacements. The area of (110) plane as well as the distance between the (110) plane and the neighboring (110) plane are fixed for these intermediate structures at a fixed volume. The results are presented in Figs. 6, 7, and 8 (the contour step is 0.5 mRy/cell). At $V=V_{exp}$, Fig. 6, the contour plot indicates the bcc structure has the lowest energy in agreement with experiment. With the application of pressure, the energy of the hcp structure is lowered and there is an energy barrier between the bcc and the hcp structures (Fig.

7). The energy barrier is about 0.004 eV/atom. At the smallest volume ($V=0.71V_{exp}$), Fig. 8, corresponding to a pressure of 38.4 kbar, the energy barrier is gone and the bcc phase no longer corresponds to a metastable structure.

To ensure a maximum cancellation of errors due to the different k-space sampling for different structures, we calculated the total energy verses atomic volume curve for bcc and hcp phases using the same k-point sampling grids under the D_{2h} symmetry (176 k-point in the IBZ, $\delta=0.0$ and $\theta=109.47°$ corresponding to the bcc structure, $\delta=\sqrt{2}/12a$ and $\theta=120.0°$ corresponding to the hcp structure, the c/a ratio 1.565 for the hcp structure was used). The calculated lattice constant, cohesive energy for bcc Ba differ from previous results[18] by less than 0.1% and the bulk modulus difference is 0.003 Mbar. The calculated bulk properties of hcp Ba are listed in table 2.

Discussion and Conclusions

The divalent alkaline-earth metals exhibit a number of interesting properties. The most striking one is the different crystal structures they exhibit as a function of temperature and pressure. The amount of d occupation increases with pressure and it has been correlated with the volume-dependent fcc- to bcc-phase transition in Ca and Sr.[7] The d occupation for Ba at ambient pressure is greater than for Ca and Sr so that the bcc phase of Ba is the stable P=0 structure. The band structures and the densities of states of bcc Ba (at $V=V_{exp}$ and under pressure, Figs. 2 and 3) indicate that the amount of d occupation

increases with pressure and the pictures in Figs. 6, 7, 8 indicate that increasing pressure favours stabilizing the hcp structure in Ba. H. L. Skriver related the bcc-hcp transition to the increasing d occupation.[7] Since the relaxation of 5p states was important for bulk calculations, we examined the effect of 5p states in phonon calculations by treating the 5p states first as the valence states and then as the core states. The calculated results are listed in Table 3. Without compression, (and under negative pressure), the same results were obtained for both cases, so the contributions of the 5p levels are not important. However, under compression, the results are quite different: the phonon frequency decreases with increasing pressure for the relaxed 5p states case and the phonon frequency remains almost a constant in a wide pressure range in the unrelaxed 5p states case. The band structures are essentially identical for both cases without compression and under compression. It seems that there is no d-occupation difference to cause the different phonon behaviour. This indicates that although the s-d transfer is in favor of lowering the energy of the hcp structure, the relaxation of the 5p states does play an important role in softening the T_1 N-point phonon and lowering the energy barrier between the bcc and the hcp phases. The 5p states should not be considered rigid core states under the compression.

From the total energy verses volume curves for bcc and hcp structures, a 0.72 cm^3/mol change in volume is predicted at the transition, in good agreement with experiment.[6] The calculated thermal transition pressure is 11 kbar (which corresponding to the enthalpies of the bcc and the hcp phase are equal for T=0 K). At low temperature

the system would not be able to overcome the energy barrier and the bcc phase would be expected to remain metastable until the T_1 N-point phonon became soft at 31 kbar. It is difficult to make a direct comparison with the experiments which have been performed at room temperature and above because of the entropy term which must be included in the free energy. Nevertheless, we suspect that the pressure at which the two enthapies are equal as predicted by theory (for T=0 K) is too low, and that some downward shift of about a fraction of a mRy per atom of the total energy of the hcp phase relative to the bcc phase may be required to bring the theory into agreement with experiment. At this stage of development of the density functional theory such an error between the ground state energies of two phases is not unlikely.

In summary, we have used first principles total energy calculations to study the pressure induced bcc to hcp phase transition in Ba. The transition path has been established and the prediction of the frequency of T_1 N-point phonon decreasing with pressure has been made. We expect that similar calculations and further experiments in the future will contribute substantially to our understanding of structural phase transitions.

References

[1]See for example, A. G. Khachaturyan, Theory of Structural Transformations in Solid (John Wiley and Sons, New York, 1983).

[2]J. W. Christain, The Theory of Transformations in Metals and Alloys, second edition (Pergamon, Oxford, 1975).

[3]K. Takemura and K. Syassen, J. Phys. F 15, 543 (1985).

[4]D. J. Decker, W. A. Bassett, L. Merrill, H. T. Hall, and J. D. Barnett, J. Phys. Chem. Ref. Data 1, 773-836 (1972).

[5]A. Jayaraman, W. Klement, Jr. and G. C. Kennedy, Phys. Rev. Lett. 9, 387, (1963); (A slope ~ 22 K/kbar was suggested for the bcc Ba to the BaII transition). J. F. Cannon, J, Phys. Chem. Ref. Data 3, 792 (1974).

[6]P. W. Bridgman, Proc. Am. Acad. Arts Sci. 74, 425 (1942); Phys. Rev. 60, 351 (1941).

[7]H. L. Skriver, Phys. Rev. Lett. 49, 1768 (1982).

[8]A. O. E. Animalu, Phys. Rev. 161, 445 (1967).

[9]W. G. Burgers, Physica I, 561 (1934); also, A. Nagasawa, N. Nakanishi, and K. Enami, Philos. Mag. A 43, 1345 (1981).

[10]See for example, C. Stassis and J. Zarestky, Solid State Commun. 52, 9 (1984).

[11]P. Hoberberg, W. Kohn, Phys. Rev. 136, 16 B864 (1964); W. Kohn and L. J. Sham, Phys. Rev. 140, A1133 (1965).

[12]L. Hedin and B. I. Lundqvist, J. Phys. C 4, 2064 (1971).

[13]M. Born and R. Oppenheimer, Ann. Phys. (Leipzig) 84, 457 (1927).

[14]D. R. Hamann, M. Schluter, and C. Chiang, Phys. Rev. Lett. 43, 1494 (1979).

[15]M. T. Yin and M. L. Cohen, Phys. Rev. Lett. 45, 1004 (1980) and Phys. Rev. B 26, 3259, 5668 (1982); P. K. Lam and M. L. Cohen, Phys. Rev. B 24, 4224 (1981).

[16]K.-M. Ho, C.-L. Fu, and B. N. Harmon, Phys. Rev. B 29, 1575 (1984).

[17]S. G. Louie, K.-M. Ho, and M. L. Cohen, Phys. Rev. B 19, 1774 (1979).

[18]Y. Chen, K.-M. Ho, B. N. Harmon and C. Stassis, Phys. Rev. B 33, 3684, (1986).

[19]The 4% discrepancy with the lattice constant is larger than for more strongly bonded crystals, partly because the total energy of the crystal changes very little as a function of volume as evidenced by the small bulk modulus. This discrepancy is consistent with results found by other workers for Ca and Sr (J. P. Jan and H. L. Skiver, J. Phys. F 11, 805 (1981)), and might be attributed to errors due to the local density approximation.

[20]W. B. Pearson, A Handbook of Lattice Spacings and Structures of Metals and Alloys (Pergamon Press, New York, 1967), Vol. 2.

[21]K. Gschneidner, Jr., in Solid State Physics, edited by F. Seitz, D. Turnbull, and H. Ehrenreich (Academic, New York, 1964), Vol. 16, 308.

[22]L. Brewer, Lawrence Berkeley Laboratory Report, No. 3720, 1977 (unpublished).

[23]See Ref. 18, the experimental values were obtained under a pressure of 62 kbar at room temperature.

[24]J. Mizuki, Y. Chen, K.-M. Ho, and C. Stassis, Phys. Rev. B 32, 666 (1985).

[25]B. Vasvari, A. O. E. Animalu, and V. Heine, Phys. Rev. 154, 535 (1967).

[26]For a discussion of the frozen phonon method and applications to transition metals see Ref. 16.

[27]The calculated total energy of bcc Ba crystal as a function of atomic volume was fitted to the universal binding curve proposed by J. H. Rose, J. Ferrante, and J. R. Smith (Phys. Rev. Lett. 47, 675 (1981)). Then the pressure P(V)=dE/dV as a function of volume can be determined which is the entire first-principles result.

Table 1. Eigenvalues and excitation energies of the pseudoatom for different atomic configurations of Ba. The values in the parentheses denote the deviations from the corresponding all-electron results

Ba Configuration	Eigenvalues (Ry)				Excitation Energy (Ry)
	5p	5d	6s	6p	(ΔEtot)
$5s^2$	-1.3869	-0.1630	-0.2522	-0.1023	0.0
	(0.0000)	(0.0000)	(0.0001)	(-.0029)	
$5s^1 5d^1$	-1.2994	-0.1137	-0.2224	-0.0853	0.0997
	(0.0027)	(0.0002)	(-.0006)	(-.0020)	(0.0003)
$5d^2$	-1.2429	-0.0856	-0.2049	-0.0781	0.2144
	(0.0051)	(0.0000)	(-.0014)	(-.0017)	(0.0015)

Table 2. Comparison of the calculated bulk properties for bcc and hcp Ba. Also included are the selected phonon frequencies for bcc Ba along with the experimental values. The frozen phonon calculations were made using the experimental lattice constant

Bulk Properties	Lattice constant (Å)		Bulk modulus (Mbar)	Cohesive energy (eV)
bcc Ba				
Calculation	4.8		0.11	2.01[20]
Experiment	5.00[20]		0.105[21]	1.90[22]
hcp Ba	a	c		
Calculation[23]	4.3	6.73	0.11	2.0
Experiment[23]	3.901	6.155	--	--

Phonon frequencies of bcc Ba	q=(0,0,1/2) L phonon (THz)	q=(0,0,1/2) T phonon (THz)	q=(0,0,1) H-point phonon (THz)
Calculation[24]	1.38	1.55	2.20
Experiment[24]	1.22±0.12	1.52±0.04	2.15±0.07

Table 3. Comparision of the calculated T_1 N-point phonon frequencies for the relaxed and the frozen 5p states calculations. The imaginary phonon frequencies were denoted by the energy difference $\Delta E=E(\delta=0.01\sqrt{2}\ a)-E(\delta=0.0)$

Atomic Volume (a.u.)	Phonon Frequencies (THz) Calculation while 5p states were treated as valence states	Calculation while 5p states were treated as core states
440.00	0.72	0.72
421.771 (V_{exp})	0.70	0.70
334.57	0.38	0.80
297.40	$\Delta E=-1.x10^{-5}$ Ry	0.81
280.00		0.59
260.00	$\Delta E=-1.64x10^{-4}$ Ry	$\Delta E=-6.6x10^{-5}$ Ry

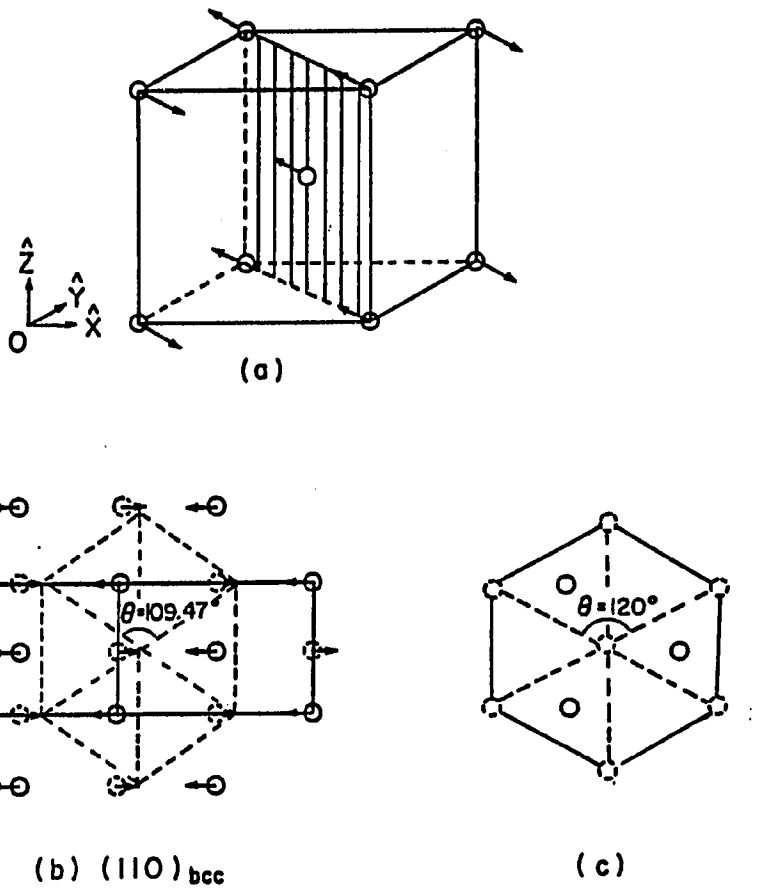

Fig. 1. The bcc-hcp phase transition coordinates

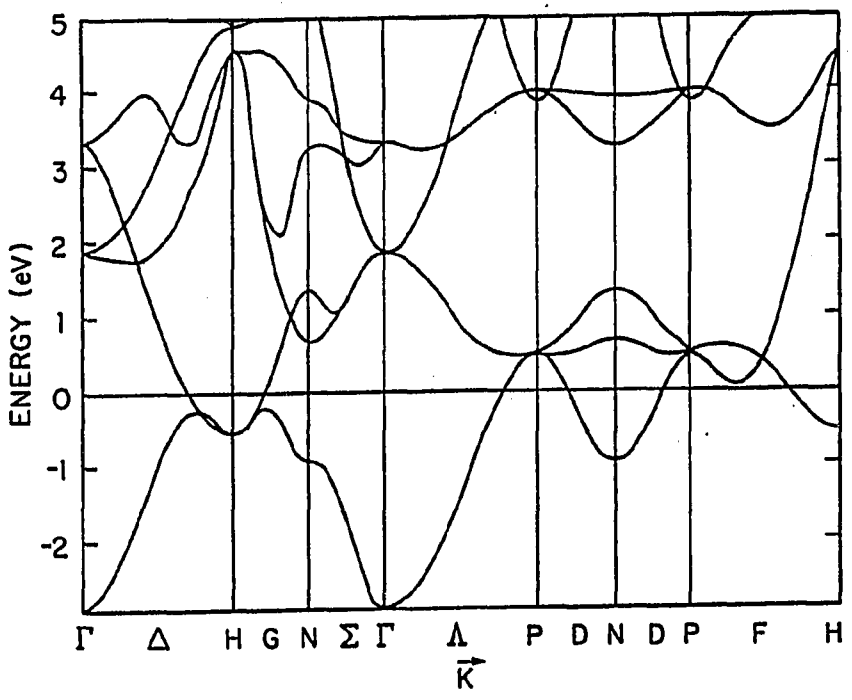

Fig. 2. The energy bands of bcc Ba calculated at the experimental volume

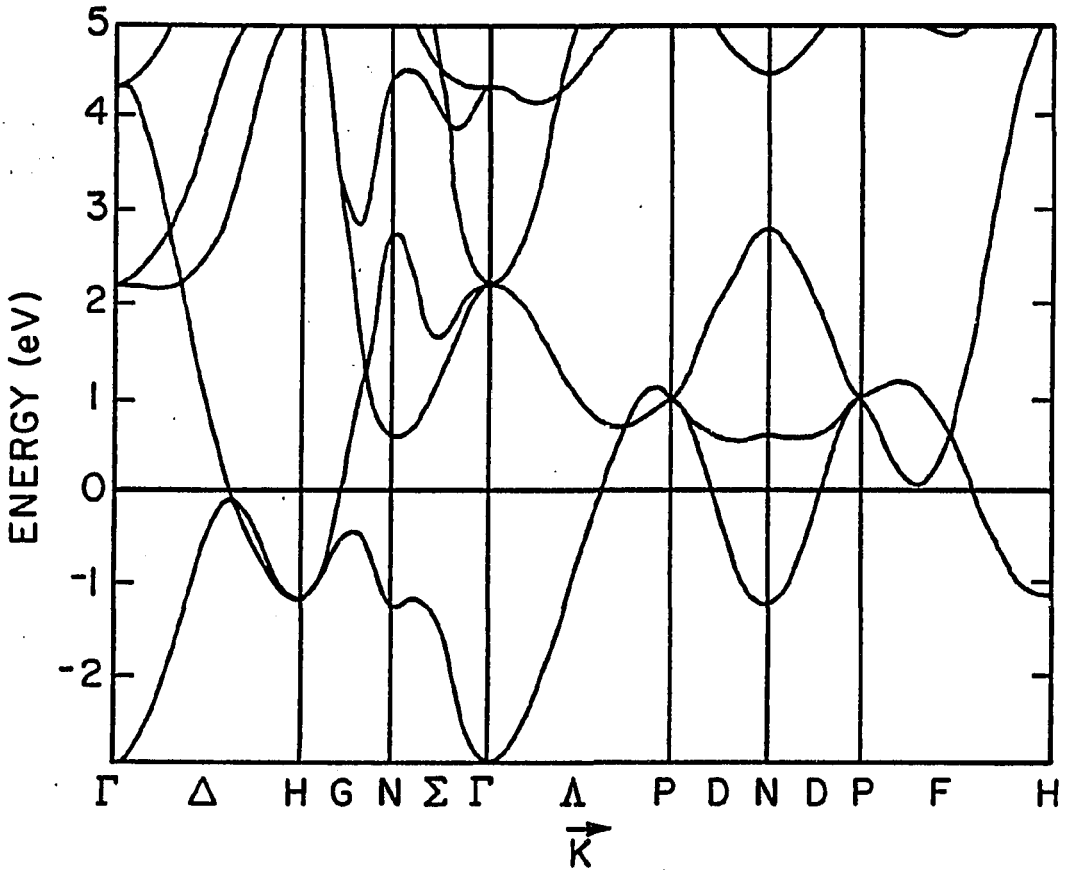

Fig. 3. The energy bands of bcc Ba calculated at $V=0.71V_{exp}$

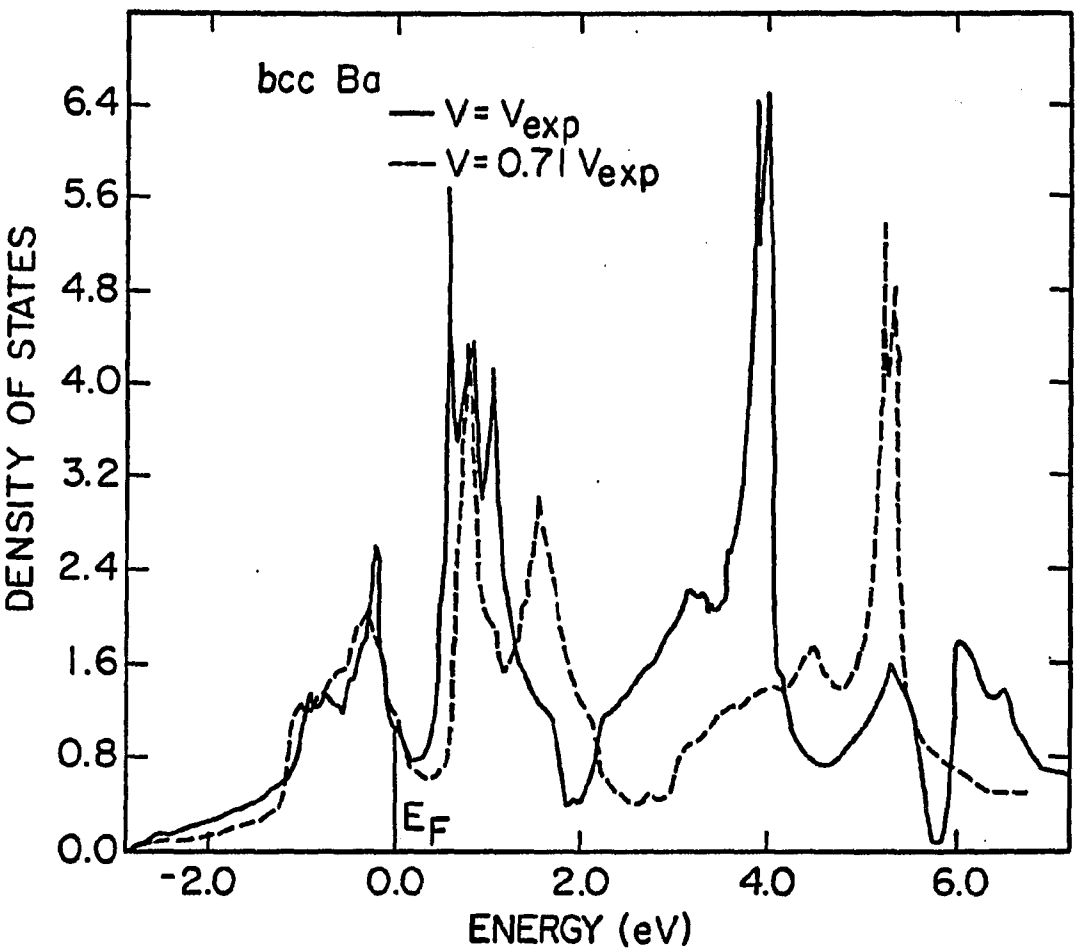

Fig. 4. The density of states for bcc Ba at the experimental volume. The dashed curves is the result from calculations at $V=0.71V_{exp}$, with the energy shifted to align the Fermi energy with the $V=V_{exp}$ result

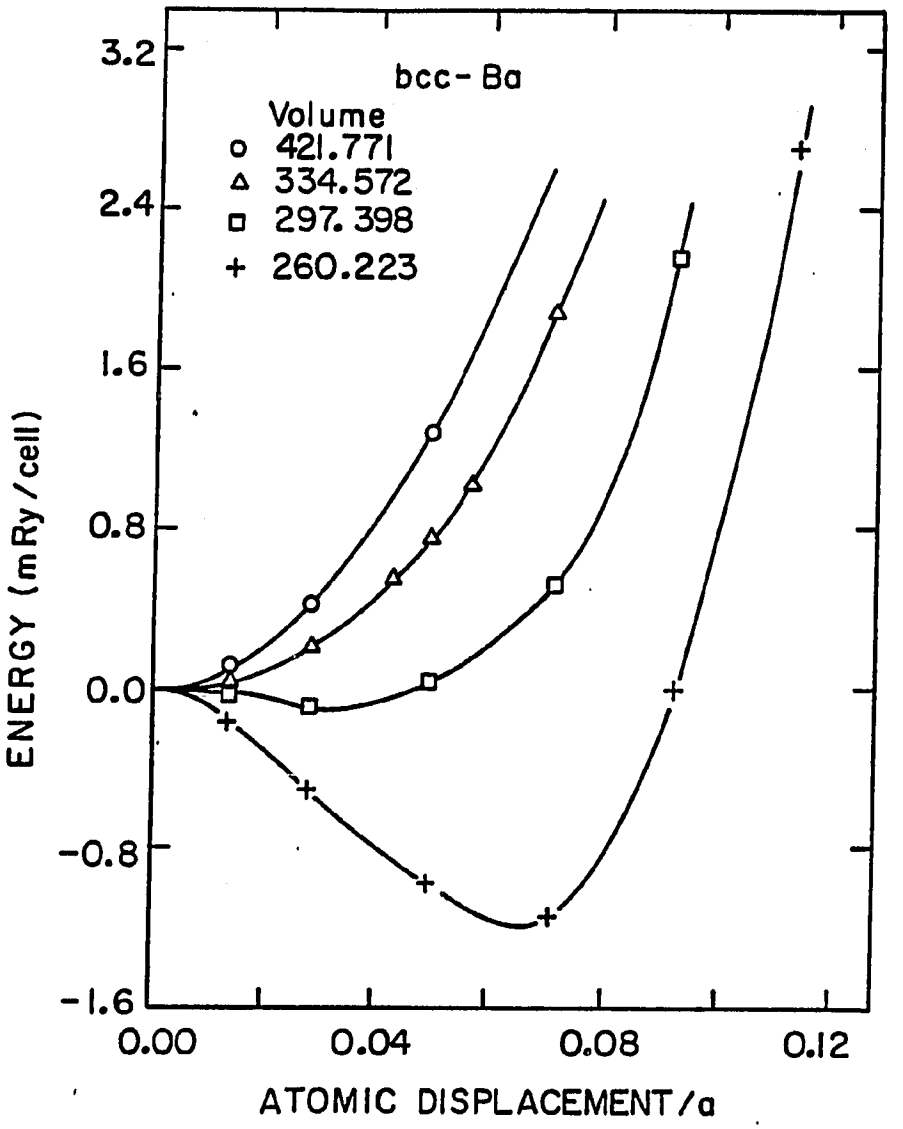

Fig. 5. The total energy vs displacement for lattice distortions corresponding to the transverse T_1 phonon mode at N point for different volumes

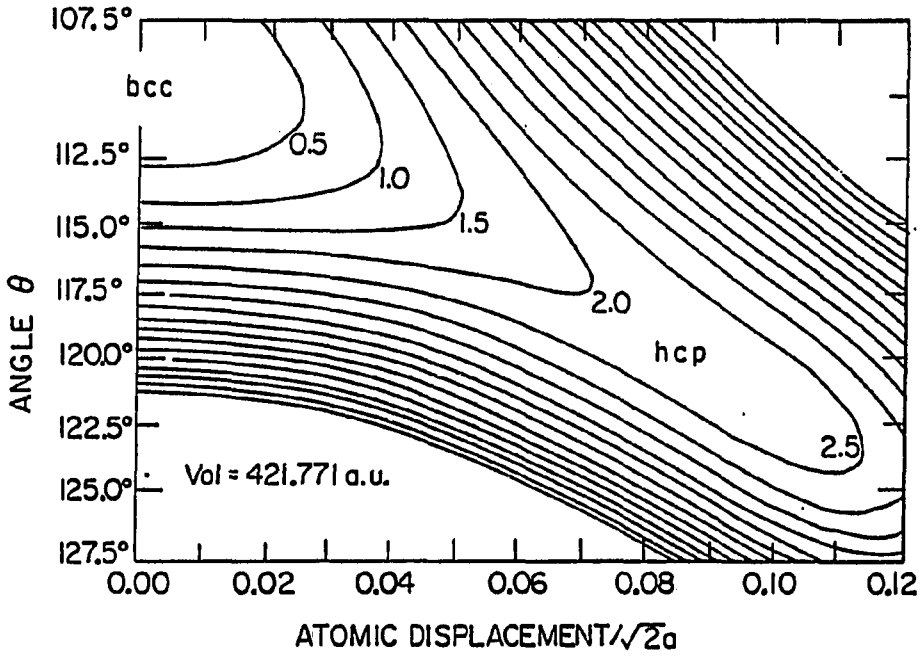

Fig. 6. The contour plot of the calculated total energy as a function of the atomic displacement corresponding to the T_1 N-point phonon mode and the angle of the shear motion at the experimental volume. The contour step is 0.5 mRy/cell

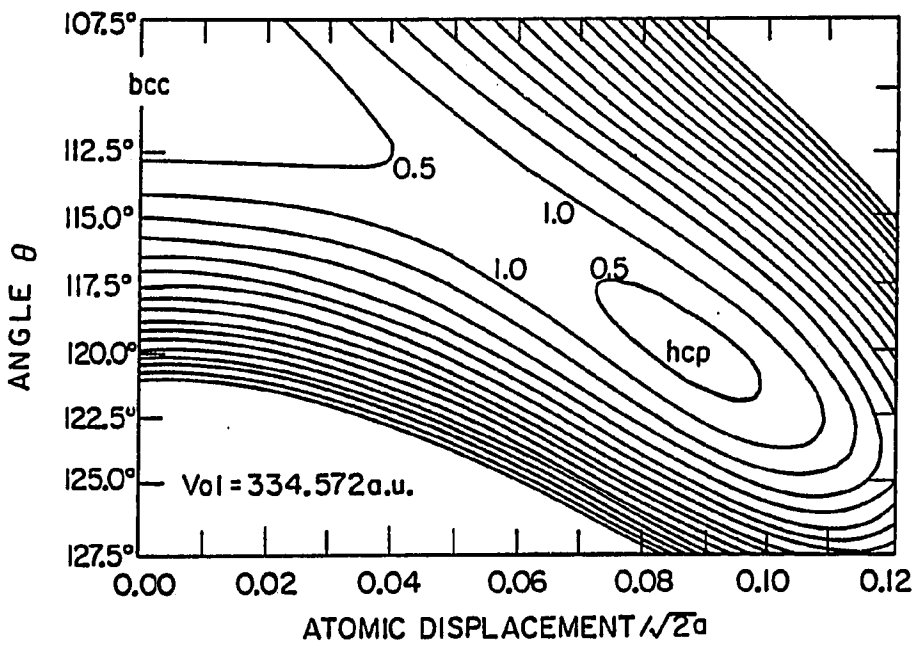

Fig. 7. Similar to Fig. 6 for V=334.572 a.u.

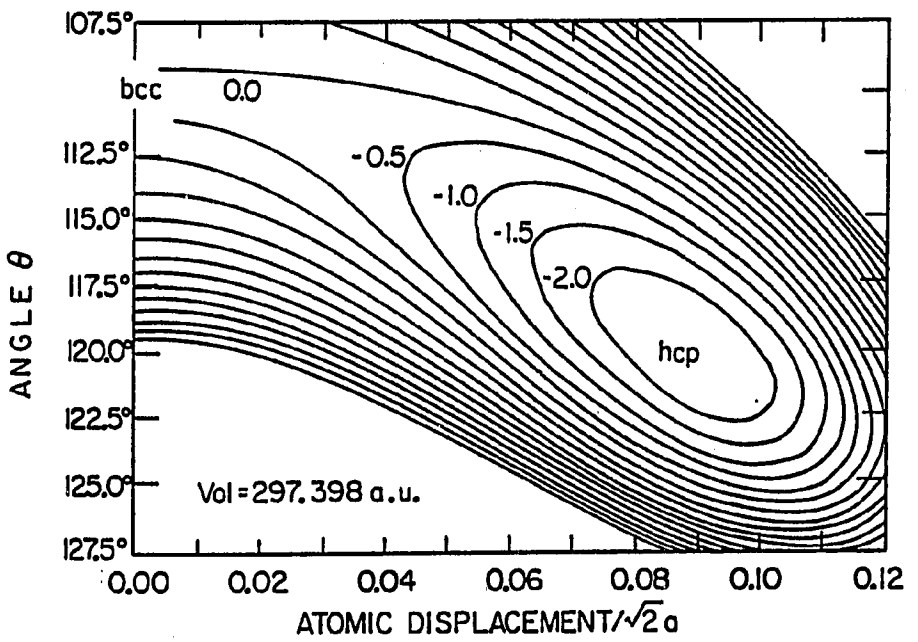

Fig. 8. Similar to Fig. 6 for V=287.398 a.u.

SECTION IV. CALCULATIONS FOR THE TRANSVERSE N-POINT PHONONS IN bcc Zr, Nb, AND Mo

Introduction

The transverse T_1 phonon branches along the [110] direction of the high-temperature bcc phases of La and Zr have recently been measured.[1] These branches have a very low frequency, reaching at the zone-boundary N point only 1.0 THz for Zr and 0.4 THz for La. At the zone center this branch is associated with the $(c_{11}-c_{12})/2$ elastic constant, and it was the small value of this elastic constant that led Zener[2] more than 30 years ago to suggest that the whole T_1 branch was low and was the source of the large vibrational entropy needed to stabilize the bcc phase at high temperatures. The T_1 mode at the zone-boundary N point is particularly interesting since the displacements for this mode take the bcc lattice in the direction of the hcp phase (with only an additional small shear required to complete the transformation).[3] Both La and Zr do in fact have low-temperature hexagonal close-packed phases. This particular mode in bcc La and Zr has also been observed to have a relatively high intensity from incoherent elastic scattering, and is expected to have a large phonon population at ~1200 K (e.g., $k_BT/\hbar\omega \sim 60$ for the T_1 branch of La), both of which suggest that anharmonic effects may play a role in stabilizing the bcc phase and causing the phase transition. The transverse modes at the N point are also unusual in Nb and Mo, the bcc metals following Zr in the periodic table. For Nb, the T_1 and T_2 frequencies are 3.9 and 5.1 THz,

respectively, while for Mo this ordering is reversed with the T_2 frequency at 4.6 THz and T_1 at 5.7 THz.

In this Brief Report, we apply the first-principles frozen-phonon method to study the N-point vibrational modes in Mo, Nb, and bcc Zr. We have previously studied, with some success, the H point and the $q=L(2/3,2/3,2/3)2\pi/a$ modes in these metals using the same methods.[4] The procedure is to calculate the total energy of the distorted crystal with atomic displacements corresponding to a particular phonon. The total energy for different magnitudes of the lattice distortion is precisely evaluated using modern self-consistent band-theoretical techniques (in this case a first-principles pseudopotential method with a mixed basis of Gaussian and plane-wave functions[5]). The only approximations entering the calculations are the standard exchange-correlation potential from local density functional theory,[6] the frozen-core approximation, and the Born-Oppenheimer approximation,[7] which provides the justification for "freezing" the phonon. From the total energy versus distortion curves, the harmonic phonon frequency can be obtained, along with information about anharmonicity and lattice stability.[4]

Calculations and Results

Before performing extensive calculations on distorted lattice lattice to obtained phonon frequencies, we tested the programs, the adequacy of the basis, and the potential for each element, by first evaluating the total energy for several different bcc unit-cell

volumes. These calculations yield the equilibrium lattice constant, bulk modulus, and cohesive energy of the crystal. The results for Nb and Mo have been reported previously[8] and we include those in Table 1[8-15] along with new results for bcc and hcp Zr, which show excellent agreement with experiment for the hcp phase and reasonable agreement for the high-temperature bcc phase (note that thermal expansion effects were not included in the theoretical treatment). The calculational procedures used for Zr were the same as those used for Nb and Mo,[8] except that there were two sets of Gaussian functions. We used one set to aid convergence of the 4d orbitals, and another for the rather extended 4p core orbitals, which in these calculations were treated as valence states. With the 4p orbitals as valence states, the equilibrium lattice constant was expanded by 2% over that obtained when the 4p orbitals were treated as core states. For the zone-boundary phonon calculations, where local changes in volume during distortion are less important, the 4p orbitals were evaluated at the smaller equilibrium volume. This results in a small shift (< 5%) in the calculated frequencies.

The good results for the calculated bulk properties with the undistorted lattice allowed us to proceed with the phonon calculations with some confidence. With distortions of the crystal corresponding to the N-point phonon displacements, the original cubic symmetry of the bcc lattice is reduced to D_{2h} (8 group operations), and the real-space unit cell is doubled. For some of the calculations, the energy for the distortion converged slowly with respect to the number of k points sampled, and as many as 612 k points in the irreducible 1/8th Brillouin

zone were employed. This difficulty in converging some of the phonons at the N point is probably related to the observation made by Varma and Weber,[16] who found that strong interband electron-phonon matrix elements for these modes occur in a rather small region in the Brillouin zone. A more complete account of the calculational details will be published in a longer paper (for details of the method see Ref. 4).

The calculated total energy versus displacement curves for the T_1 (polarization, $e_{\parallel}\langle 110\rangle$) and T_2 ($e_{\parallel}\langle 001\rangle$) modes are shown in Fig. 1 for Nb and Mo. For small displacements, the quadratic part of the curves may be used to obtain (via $E=1/2m\omega^2\delta^2$) the harmonic frequencies in Table 2.[1,17-18] The calculated frequencies are in reasonably good agreement with experiment, and display the same reversal of the T_1 and T_2 modes found experimentally. This reversal was previously shown by Varma and Weber[16] to arise from details of the electronic structure. The corresponding total energy curves for bcc Zr are shown in Fig. 2. The negative curvature for the T_1 curve indicates the bcc phase (at T=0 K) is unstable for displacements associated with the T_1 mode, while the phonon frequency of the T_2 mode is again in reasonable agreement with experiment. The longitudinal N-point phonon frequency for bcc Zr was also calculated (3.9THz) and found to be in good agreement with the experimental value (4.2 THz). The large temperature (1340 K) at which the phonon frequencies were measured for bcc Zr would normally lead to a softening of the lattice and measured frequencies somewhat below the calculated values. However, the T_1 curve for Zr indicates that the situation is more complex.

Discussion

The total energy calculations showing the instability of bcc Zr for displacements corresponding to the zone-boundary T_1 mode (Fig. 2) represent a significant step in understanding the bcc-to-hcp phase transition in this class of materials.[19] In the past, the transition to the high-temperature bcc phase was frequently explained by the nearly tautologous remark that the entropy of the bcc phase was higher. Zener[2] and Friedel[20] have speculated on the source of the required excess vibrational entropy (over that the lower temperature phase), but there has been little progress toward a detailed microscopic understanding of the phase transition. Iizumi has used neutron scattering to look for soft-mode behavior of the low-lying N-point T_1 mode in the high-temperature bcc phase of thallium, which also exhibits a hcp-to-bcc transition, but he did not detect any discernible temperature dependence of the phonon frequency, or any conspicuous change of the elastic scattering.[21] Based on the calculations presented above, and the available experimental data, we may speculate a bit further than Iizumi as to the nature of the transition. For those metals possessing a low T_1 branch in a high-temperature bcc phase, we believe the situation is similar to the case of solid helium, where the crystal structure is unstable within the harmonic approximation, but because of large displacements and attendant anharmonic effects, the lattice is stabilized. Calculations for the vibrational modes of the bcc phase would then require some form of renormalized or self-consistent phonon theory.[22] The ingredients

require to implement such theories are the anharmonic mode coupling strengths which are extractable, in principle, from frozen phonon calculations, and will be the subject of a future publication.

References

[1]C. Stassis and J. Zarestky, Solid State Commun. 52, 9 (1984).

[2]C. Zener, Elasticity and the Anelasticity of Metals (Univ. of Chicago Press, Chicago, 1948), p. 37.

[3]W. G. Burgers, Physica 1, 561 (1934); also, A. Nagasawa, N. Nakanishi, and K. Enami, Philos. Mag. A 43, 1345 (1981).

[4]K.-M. Ho, C. L. Fu, and B. N. Harmon, Phys. Rev. B 29, 1575 (1984).

[5]S. G. Louie, K.-M. Ho, and M. L. Cohen, Phys. Rev. B 19, 1774 (1979).

[6]L. Hedin and B. I. Lundqvist, J. Phys. C. 4, 2064 (1971).

[7]M. Born and R. Oppenheimer, Ann. Phys. (Leipzig) 84, 457 (1927).

[8]C. L. Fu and K.-M. Ho, Phys. Rev. B 28, 5480 (1983).

[9]Properties and Selections: Nonferrous Alloys and Pure Metals, Metals Handbook, 9th ed. (American Society of Metals, Cleveland, 1979), Vol. 2.

[10]J. M. Dickinson and P. E. Armstrong, J. Appl. Phys. 38, 602 (1967).

[11]L. Brewer, Lawrence Berkeley Laboratory, Report No. 3720, 1975 (unpublished).

[12]W. C. Hubbell and F. R. Brotzen, J. Appl. Phys. 43, 3306 (1972).

[13]The experimental value of the lattice constant is for T=862 °C [Lattice Spacings and Structures of Metals and Alloys, edited by W. B. Pearson (Pergamon, New York, 1967), Vol. 2] while the theoretical value is strictly valid only at T=0 K, so that the difference between the calculational and experimental values involves thermal expansion effects.

[14]J. Goldak, L. T. Lloyd, and C. S. Barrett, Phys. Rev. 144, 474 (1966).

[15]E. S. Fisher, M. H. Manghnani, and T. J. Sokolowski, J. Appl. Phys. 41, 2991 (1970).

[16]C. M. Varma and W. Weber, Phys. Rev. Lett. 39, 1094 (1977); Phys. Rev. B 19, 6142 (1979).

[17]B. N. Powell, P. Martel, and A. D. B. Woods, Phys. Rev. 171, 727 (1968).

[18]C. Stassis, J. Zarestky, and N. Wakabayashi, Phys. Rev. Lett. 41, 1726 (1978).

[19]Similar calculations on the high-temperature bcc phase of La show the same instability and will be reported elsewhere.

[20]J. Friedel, J. Phys. (Paris) Lett. 35, L59 (1974).

[21]M. Iizumi, J. Phys. Soc. Jpn. 52, 59 (1983).

[22]See, for example, Dynamics of Perfect Crystals, edited by G. Venkataraman, L. A. Feldkamp, and V. C. Sahni (M.I.T. Press, Cambridge, MA, 1975), Sec. 7.2; Thermodynamics of Crystals, edited by D. C. Wallace (Wiley, New York, 1972), Sec. 14.

Table 1. Comparison of calculated and measured values for the static bulk properties of Mo, Nb, and Zr

	Lattice constant (Å)		Bulk modulus (Mbars)	Cohesive energy (eV/atom)
Mo				
Calculated	3.14[a]		2.85	6.64
Experiment	3.14[b]		2.62[c]	6.82[d]
Nb				
Calculated	3.26		1.82	7.55
Experiment	3.29[b]		1.735[e]	7.57[d]
bcc Zr				
Calculated	3.54[f]		1.05	6.93
Experiment	3.61[f]		...	...
hcp Zr	a	c		
Calculated	3.20	5.13	1.01	6.98
Experiment	3.23[g]	5.14[g]	0.95[h]	6.25[d]

[a]Reference 8.
[b]Reference 9.
[c]Reference 10.
[d]Reference 11.
[e]Reference 12.
[f]Reference 13.
[g]Reference 14.
[h]Reference 15.

Table 2. Comparison of the calculated and measured values for the frequecies of the N point, $(1,1,0)\pi/a$, transverse vibrational modes in Mo, Nb, and the high-temperature bcc phase of Zr. The theoretical values are converged to ±0.1THz

	T_1, (e_u<110>) (THz)	T_2, (e_u<001>) (THz)
Mo		
Calculated	5.8	4.0
Experiment	5.73±0.06[a]	4.56±0.06[a]
Nb		
Calculated	4.3	5.1
Experiment	3.93±0.06[a]	5.07±0.10[a]
bcc Zr		
Calculated	Unstable	3.6
Experiment	1.00±0.05[b]	3.94±0.07[c]

[a]Reference 17.

[b]Reference 1.

[c]Reference 18.

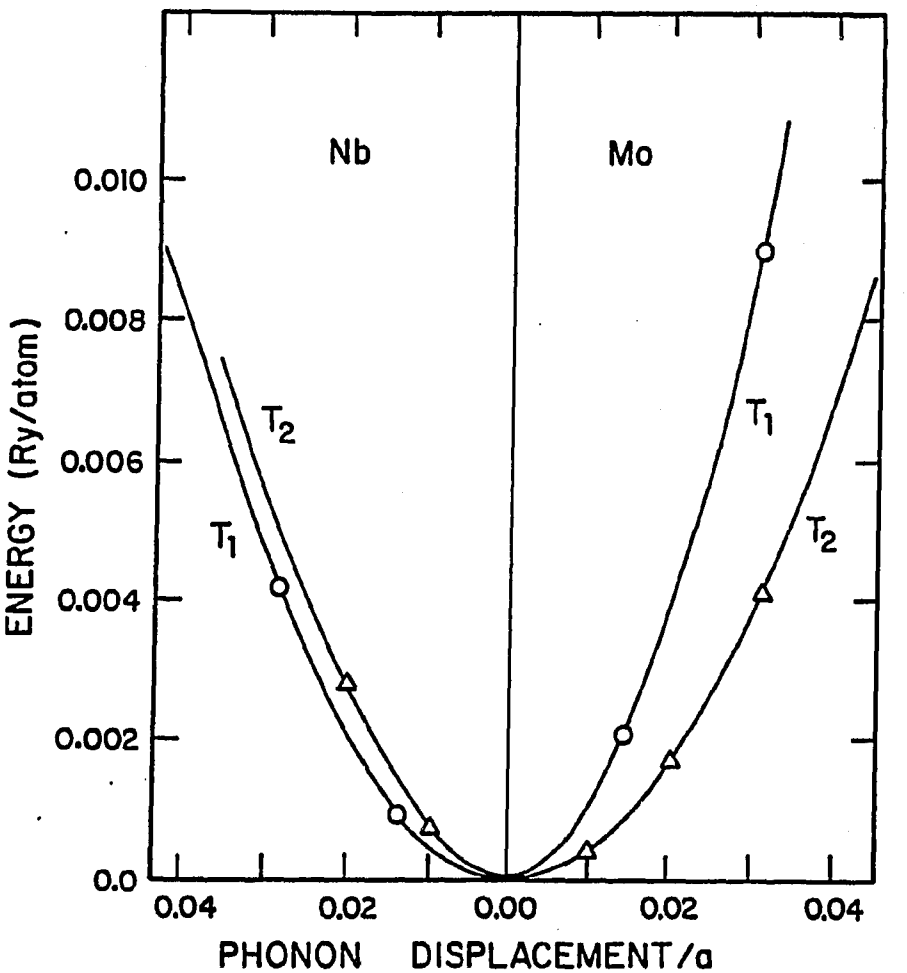

Fig. 1. The total energy vs displacement for lattice distortions corresponding to the two transverse-phonon modes at the N-point. Because of symmetry, the curves are symmetric about zero displacement, so only positive displacements are shown for Mo, and negative for Nb

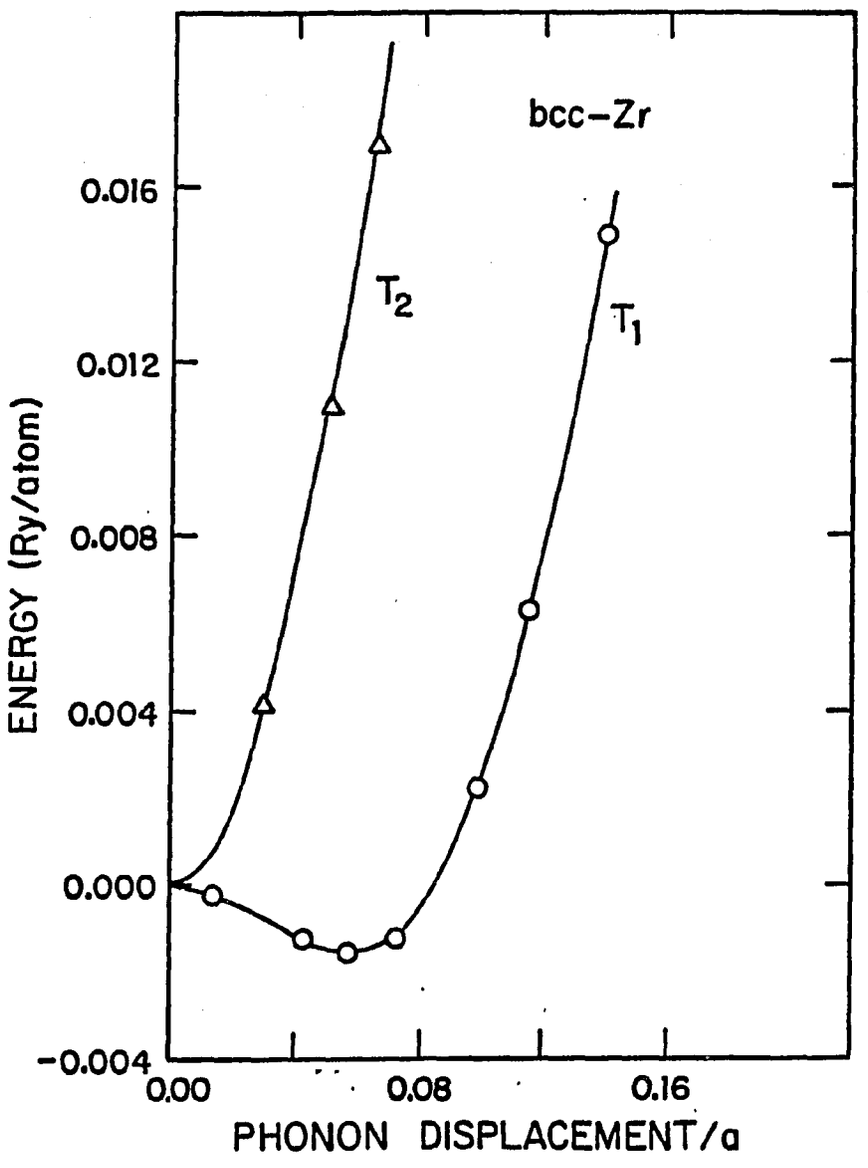

Fig. 2. Similar to Fig. 1 for the bcc phase of Zr

SECTION V. PHONON-PHONON COUPLING AND THE STABILITY OF THE HIGH TEMPERATURE bcc PHASE OF Zr

Introduction

There has recently been renewed interest in the stability of phases separated by a first order temperature dependent phase transition. Insights have been obtained by the use of simple statistical models and by computer simulations[1,2]; however, for specific materials a more detailed microscopic picture is generally lacking and needed. We show for an important class of transitions that such a microscopic picture can be obtained through modern first principles electronic structure calculations.

Increases in computing speed have made feasible the first principles calculation of many material dependent properties - including vibrational frequencies, bulk moduli, cohesive energies, and phase transition pressures. These calculational methods are based on the very precise evaluation of the total energy changes associated with atomic displacements in crystals. Unlike traditional perturbative methods, these calculations are not restricted to small distortions of the crystal. This enables the accurate determination of anharmonic interactions as well as coordinate paths and barrier heights for phase transitions. Until recently this anharmonic information has not been analyzed, with the notable exception of the calculation of the optical mode frequency shift caused by the two phonon process in diamond.[3] In this paper we use the anharmonic terms derived from accurate total

energy calculations to obtain phonon-phonon coupling strengths for the high temperature bcc phase of Zr. The temperature dependence of the lattice vibrational modes are determined and the interactions responsible for the high temperature stability of the bcc phase are identified.

It has been noted that many elements crystallize in the bcc structure when cooled from the melt, although at low temperatures their crystal structure is not bcc.[4,5] Several investigators have speculated on the origin of the extra entropy which is required to stabilize the bcc phase at high temperatures. Based on the small shear restoring forces observed for some of these elements in the bcc phase Zener proposed the larger entropy arose from a low energy transverse phonon branch,[6] while Friedel using a simplified tight binding model argued that the higher entropy was associated with the topology (fewer nearest neighbors) of the bcc lattice.[4] As presented below, our investigations indicate that for Zr there is a low lying transverse shear mode which makes large contributions to the stability of the bcc phase through strong anharmonic coupling to other low frequency modes.

We have chosen to study the first order hcp-bcc transition of Zr for several reasons. First, the transition at T=1136 K is martensitic, which means the atomic positions of the parent and the resultant crystal structure are highly correlated; thus limiting the configuration coordinates which must be varied.[7] Based on the observed correlations in crystal orientations, Burgers proposed that the transition from bcc to hcp occurs through the displacements of the zone boundary T_1 N-point phonon together with a long wavelength tetragonal

mode.[8,9] Second, the phonon dispersion curves as a function of temperature for both the hcp and bcc phases have been obtained by neutron scattering experiments.[10] These experiments for the bcc phase showed that the frequencies for the entire [110] T_1 phonon branch are indeed very low. In conjunction with these experimental measurements, first principles calculations of the harmonic frequency for the T_1 N-point phonon were made.[11] These calculations yielded an imaginary frequency which indicates that within the harmonic approximation this mode for Zr is unstable. In contrast, similar calculations for the N-point phonons of bcc Nb and Mo, which are stable at low temperatures, yielded frequencies in good agreement with experimental values.[11] Thus, to understand the stability of the high temperature bcc phase of Zr and in particular the measured frequency of 1 THz for the T_1 N-point phonon it is of vital importance to include anharmonic interactions. The situation is similar to that of He for which the bcc structure is stabilized by the anharmonic forces even at zero temperature.[12]

Theoretical Methods

The total energy calculations were performed using an established first principles pseudopotential method which along with calculational procedures has been described in detail elsewhere.[13] The only approximations involve the treatment of the exchange-correlation energy using the local density functional formalism,[14] the frozen core approximation, and the Born-Oppenheimer approximation. For the analysis of a particular phonon the total energy is evaluated as a

function of atomic displacements with the atoms moving in the directions corresponding to the phonon polarization vector. These so called "frozen-phonon" calculations have been shown to be accurate for the determination of phonon frequencies in transition metals.[15] The results of such calculations for the T_1 mode of Zr are shown in Fig. 1. The insert shows the energy vs displacement curve has a minimum at finite displacements and indicates the instability toward the hcp phase. Expanding the energy in a power series in the displacement we can write $\Delta E = a\delta^2 + b\delta^3 + c\delta^4 + \ldots$. The negative harmonic coefficient, a, and the positive fourth order coefficient, c, are conveniently displayed in the $\Delta E/\delta^2$ vs δ^2 plot of Fig. 1 (b=0 by symmetry for the T_1 mode). Similar analysis was made for the T_2 and L phonons at the N-point, the H-point phonon, and the longitudinal (2/3, 2/3, 2/3) phonon (the ω-phase mode).

To determine the temperature dependence of the phonon frequencies we make use of the extensive perturbative formalism developed for the treatment of anharmonic effects in crystals.[16] As shown in Fig. 1 the total crystalline internal energy can be to a good approximation expanded through fourth order in a power series in the displacements from the bcc structure, for amplitudes relevant to the hcp transition. The harmonic approximation consists of retaining the second order terms and solving the quadratic Hamiltonian for the normal modes of vibration. The third and fourth order expansion coefficients are then rewritten in terms of these normal mode coordinates so that the anharmonic effects are treated as interactions among the elementary excitations (phonons). Our strategy is then to first obtain the volume

dependent unrenormalized harmonic frequency using first principles frozen-phonon calculations. The renormalized frequency and phonon lifetime are then obtained from the calculated anharmonic potential using the standard formulas.[17] In these formulas the temperature enters through the self-consistent phonon occupation factors.

In order to evaluate the third and fourth order coupling coefficients for all phonon interactions we assumed the anharmonic part of the interatomic interactions were short ranged (1st and 2nd nearest neighbors only) and could be modeled by a two parameter central potential of the form C/r^n. The parameters C and n were determined from a least squares fit to the 4th order expansion coefficients from frozen phonon calculations for five low lying phonons. Table 1 lists the coefficients and the corresponding values from the fit function.

The required Brillouin zone summations were performed by dividing the zone into small cubes with the phonon coupling strengths assumed constant within each cube. The frequencies appearing in the typical second order perturbation theory formulas were assumed to vary linearly within each cube and the integration involving the energy denominators was performed analytically.[18] To test convergence the number of cubes along G to H was varied between 10 and 30. The large fourth order term was fully converged even with 10 divisions, while the smaller third order term required more than 20 divisions. For computational expediency the majority of the calculations were performed with 10 divisions and the uncertainty of the third order results is ~ 20%.

Results and Conclusions

The second, third and fourth order contributions to the squared frequency at 1400K for the T_1 and T_2 N-point phonons are given in Table 2. For the T_1 mode the second and third order contributions are negative, while the fourth order contribution is larger and positive. The resulting frequency of 1 THz is in good agreement with experiment, however this may be somewhat fortuitous. The important result is the renormalization of the T_1 mode to finite frequency. The fourth order contributions responsible for the frequency shift of the T_1 mode arise predominantly from interactions with other phonons in the T_1 branch. This is evident in Fig. 2 where the k-dependent 4th order contributions are shown. A similar analysis shows that third order contributions are large in the vicinity of the G point.

Frequencies were also evaluated for a number of other phonon modes. In general the calculated frequency corrections are dominated by the positive fourth order contributions and are in the direction to bring the harmonic frequencies (from the frozen phonon calculations) into agreement with the high temperature experimental values; however the renormalized frequencies in some cases overshoot by as much as 20%. We believe this may be partly due to limitations in applying perturbation theory at such high temperatures, and possibly also due to the simple central potential approximation.

Having established that at high temperatures the bcc structure is a stable phase from the viewpoint of the finite frequency of the N-point T_1 phonon, it is instructive to consider how this stability can

be understood in terms of the free energy. At high temperatures the bcc phase is stable because of its large entropy relative to other lattice configurations. For Zr the lattice vibrational entropy accounts for ~60% of the difference between the bcc and the hcp phases (the other ~40% is from electronic contributions). We can calculate the change (decrease) of lattice entropy when the bcc structure is distorted toward the hcp phase by a small displacement corresponding to the T_1 N-point mode. We use the anharmonic coupling constants to evaluate the changes in all the phonon frequencies as the bcc crystal is distorted. The phonons whose frequencies are most affected by the T_1 distortion of the bcc crystal are those with strong positive 4th order anharmonic coupling constants (see Fig. 2). The strong 4th order coupling of the T_1-mode with other phonons raises the frequencies of these modes, leading to a decrease in the entropy. This implies that at high enough temperatures the bcc phase will be stable relative to the T_1 displacements. A similar analysis for a distortion of the bcc structure corresponding to the ω-phase displacements again shows a strong coupling to the T_1 branch is responsible for the stability of the bcc phase at high temperatures. It is interesting that Zener long ago proposed that the extra entropy needed to stabilize the bcc phase comes from soft shear modes in the bcc structure. Our investigations have confirmed this picture and singled out the T_1 branch as being most important because the phonons of this branch are low in energy and have large anharmonic coupling.

The analysis given above leads to the following microscopic picture of the first order bcc to hcp phase transition. For the

internal energy, there is a trough in coordinate space leading from the bcc down to the ground state hcp structure.[19] The relevant coordinates are the displacements corresponding to the T_1 N-point phonon (internal shear) and a uniform or long wavelength tetragonal strain. At temperatures just above the transition the bcc structure is stable and has the lowest free energy. At these temperatures the hcp structure corresponds in the free energy surface to a local minimum separated from the bcc minimum along the transition path by a low barrier. As the temperature is decreased there is a small softening of the bcc T_1 branch which lowers the free energy along the transition path and allows the hcp minimum to fall below the bcc free energy. This is consistent with the Landau theory for a weakly first order transition and a study of the transition based on a Landau expansion of the free energy has been made with the T_1 displacements and the coupled uniform tetragonal strain as coordinates.[20] There is currently much interest in precursor effects for such transitions and we have been able to calculate in addition to the small softening for the T_1 mode a temperature dependent quasielastic contribution to the neutron scattering cross section. A theoretical study of the wave vector dependence of the quasielastic linewidths is now underway. Comparison with experiment is made difficult by the extra contributions from impurities and other defects, but strong quasielastic scattering was observed under the T_1 branch in bcc Zr.[10] A more thorough experimental study of the quasielastic scattering would now seem worthwhile.

In summary, we have used first principles total energy calculations to derive phonon-phonon coupling strengths and have

established the interactions responsible for stabilizing the high temperature bcc phase of Zr. These calculations provide a concrete basis for understanding the weakly first order bcc to hcp transformation and open the door for a detailed theoretical analysis of precursor effects in a class of materials that is experimentally interesting.

References

[1]See for example, Modulated Structure Material, ed. T. Tsakalakos, NATO ASI Series, Series E: Applied Sciences No. 83 (M. Nijhoff, Boston, 1984).

[2]Phase Transformations in Solids, edited by T. Tsakalakos, Material Research Society Proceedings Vol. 21 (North-Holland, New York, 1984).

[3]D. Vanderbilt, S. G. Louie, and M. L. Cohen, Phys. Rev. Lett. 53, 1477 (1984).

[4]J. Friedel, J. de Physique - Lettres 35, L-59 (1974).

[5]S. Alexander and J. McTague, Phys. Rev. Lett. 41, 702 (1978).

[6]C. Zener, Phys. Rev. 71, 846 (1947); Elasticity and Anelasticity Metals, by C. Zener, (Univ. of Chicago Press, Chicago, 1948).

[7]In addition to the bcc to hcp transition, there is a competing transformation to the ω-phase structure which can be stabilized by pressure or alloying. References to the ω-phase can be found in S. K. Sikka, Y, K. Vohra, and R. Chidambaram, Prog. in Mat. Sci. 27, 245 (1982).

[8]W. G. Burgers, Physica (Utrecht) 1, 561 (1936).

[9]Z. Nishiyama, Martensitic Transformations (Academic Press, New York, 1978).

[10]C. Stassis, J. Zarestky, D. Arch, O. D. McMasters and B. N. Harmon, Phys. Rev. B 18. 2632 (1978); C. Stassis, J. Zarestky, and N. Wakabayashi, Phys. Rev. Lett. 41, 1726 (1978); C. Stassis and J. Zarestky, Solid State Commun. 52, 9 (1984).

[11]Y. Chen, C.-L. Fu, K.-M. Ho, and B. N. Harmon, Phys. Rev. B 31, 6775 (1985).

[12]N. R. Werthamer, Am. J. Phys. 37, 763 (1969).

[13]C.-L. Fu and K.-M. Ho, Phys. Rev. B 28, 5480 (1983).

[14]The local exchange correlation function was obtained from L. Hedin and B. I. Lundqvist, J. Phys. C 4, 2064 (1971).

[15]K.-M. Ho, C. L. Fu, and B. N. Harmon, Phys. Rev. B 29, 1575 (1984).

[16]A review of the standard formalism used to treat anharmonic crystals is given in R. A. Cowley, Rep. on Prog. in Phys. 31, 123 (1968).

[17]Equations (3.1) and (3.2) of Ref. 16. At temperatures for which the bcc phase is stable the perturbations are large, at least for the T_1 branch. For this reason self-consistency is important. On the right hand side of these equations we have therefore used the experimental $\omega(\mathbf{q})$ as the fully renormalized frequencies (equivalent to using Brillouin-Wigner perturbation theory).

[18]P.-A. LindgÅrd, Solid State Commun. 16, 481 (1975); J. Rath and A. J. Freeman, Phys. Rev. B 11, 2109 (1975).

[19]A detailed volume dependent picture of the bcc to hcp transition path has been calculated from first principles for barium. The bcc to hcp transition in barium takes place as a function of pressure. Y. Chen, K.-M. Ho, and B. N. Harmon, Department of Physics, Iowa State University, Ames, Iowa, unpublished.

[20]P.-A. LindgÅrd and O. G. Mourits, Phys. Rev. Lett. 57, (1986).

Table 1. Fourth order expansion coefficients for the three N-point and the H-point phonons along with the (2/3, 2/3, 2/3)L phonon, labelled ω. The top line gives the results from first principles calculations, while the second line gives the values obtained from the two parameter fitted function as described in the text. The units are in Ry/(A^4-atom)

	$N-T_1$	$N-T_2$	N-L	H	ω
First Principles	0.57	-0.21	1.39	-0.66	-0.21
Fit	0.37	-0.29	1.73	-0.72	-0.17

Table 2. The calculated contributions at T = 1400 K to the N-point T_1 phonon frequency squared; ν_2 is the imaginary harmonic frequency, and ν_3 and ν_4 are the 3rd and 4th order corrections. The corresponding values for the N-point T_2 mode are also given. The experimental frequencies are from Ref. 10

	ν_2^2	ν_3^2	ν_4^2	$\nu^2 = \Sigma\nu_n^2$	ν (THz)	ν_{exp}(Thz)
T_1	-3.72	-2.10	6.82	1.00	1.00	1.00±0.05
T_2	7.92	-0.80	3.18	10.30	3.20	3.88±0.15

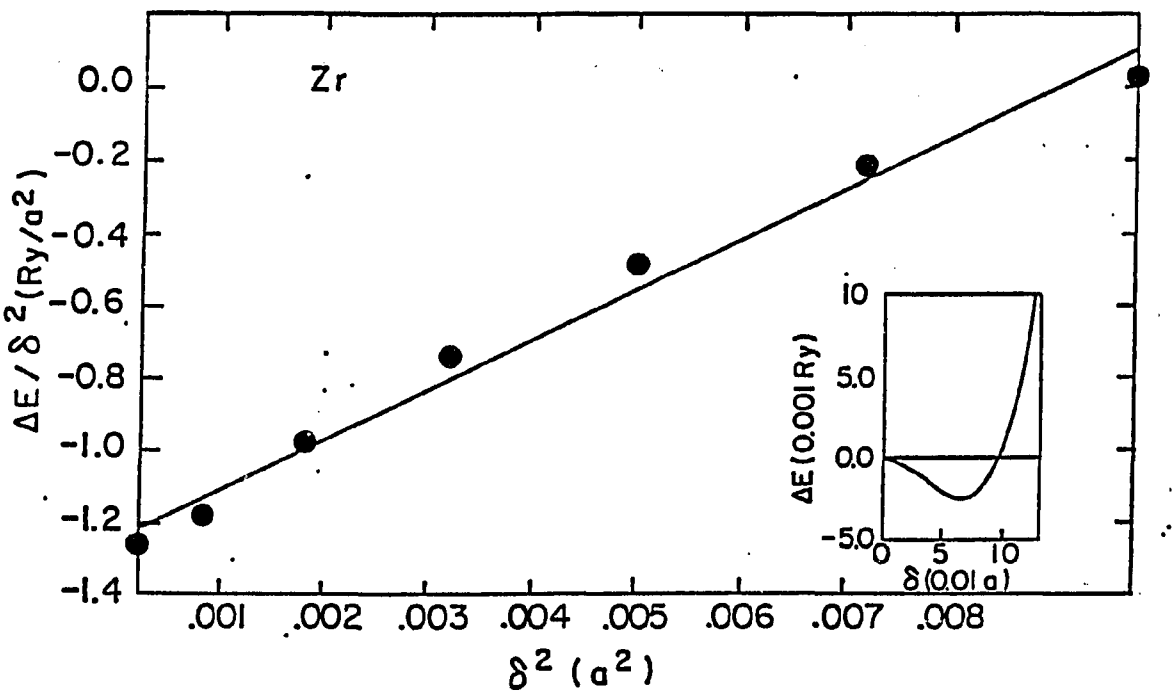

Fig. 1. $\Delta E/\delta^2$ vs δ^2 for the N-point T_1 mode. The slope of the line gives the fourth order anharmonic coefficient for the energy vs displacement expansion

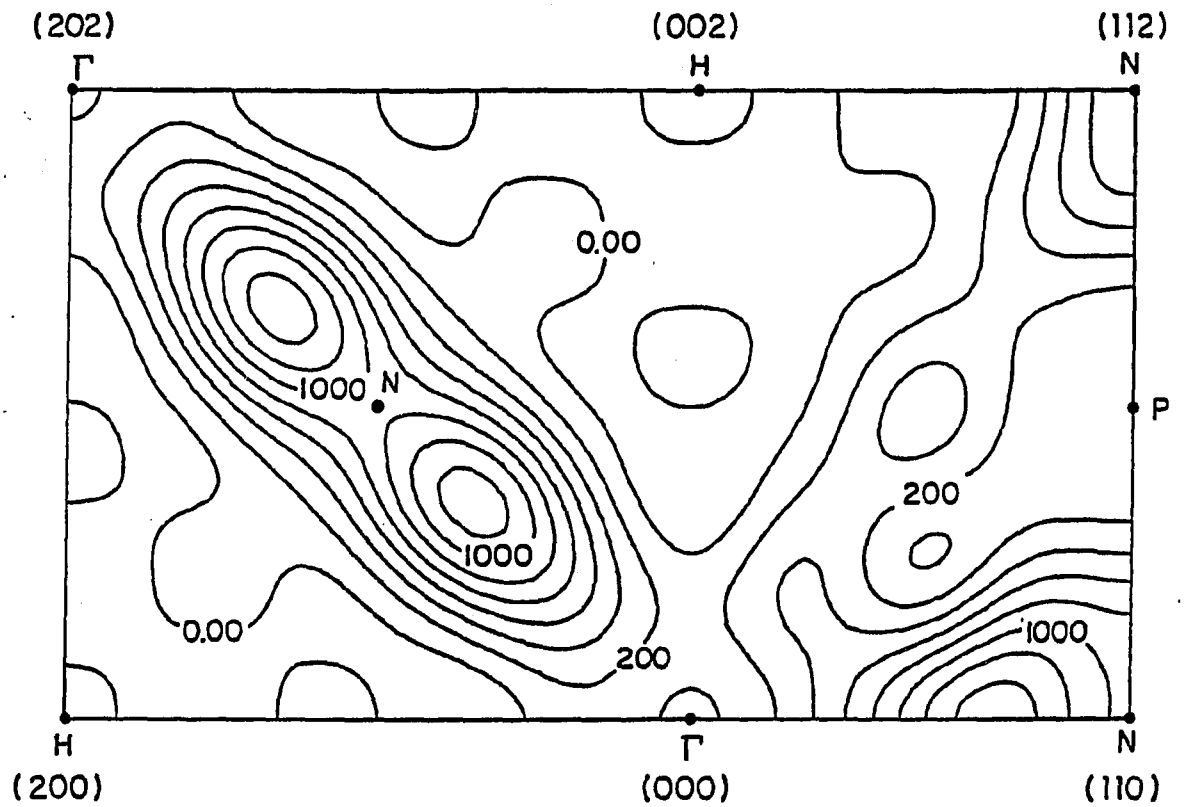

Fig. 2. Contour plot of the 4th order contributions of branch 1 to the frequency shift for the T_1 N-point phonon. The contours are shown for the high symmetry planes. The dominant contributions along the (110) direction arise from strong anharmonic coupling and high thermal occupation (Contours at intervals of 200 in arbitrary units)

SUMMARY

First-principles studies of phonon anomalies and the bcc-hcp martensitic phase transitions in Zr and Ba were presented in this thesis. In Section I, a brief description for the method of calculation is given and the use of total energy calculations to study the bulk properties for Zr in the ω, bcc, hcp, fcc structures is presented. From these calculations we obtain equilibrium lattice constants, cohesive energies, bulk moduli and the energy difference between the bcc and the hcp phases which are in good agreement with experiment. Recent neutron scattering experiment on single crystals of bcc Ba have revealed that the longitudinal branch along [100] direction is lower than the transverse branch. This is quite anomalous and does not occur in the measured dispersion curves of bcc Sr.[15] Also, the previous theoretical calculations for the phonon spectra of Ba had not predicted this unusual feature.[16] The calculations described in Section II are aimed at understanding the interactions responsible for this behavior. By performing calculations both with and without the d-states, we find that the [100] longitudinal branch is lowered because of strong interactions with the electronic states having d-like character. In Section III, the study of the pressure induced bcc-hcp transition in Ba is presented. We use the first principles technique to map out the energy path for the solid-solid phase transition and to study the pressure effect for the T_1 N-point phonon frequency. The volume dependence of the complete energy surface from the bcc to the hcp structure is determined as a function of atomic displacements

corresponding to the T_1 N-point phonon mode and a long wavelength shear. The results predict that the frequency of this phonon mode decreases with increasing pressure. In Sections IV and V, we focus on the temperature-dependent bcc-hcp transition in Zr. Frozen phonon calculational results for the T_1 N-point phonon of Zr indicate an instability toward the formation of the hcp phase with the harmonic approximation at T=0 K. The third and fourth order anharmonic coupling strengths have been determined from the frozen phonon calculations and used to evaluate the temperature dependence of selected phonon frequencies in bcc Zr. It is found that phonon-phonon interactions are crucial for stabilizing the high temperature bcc phase of Zr.

LITERATURE CITED AND NOTES

[1]See for example, A. G. Khachaturyan, Theory of Structural Transformations in Solids (Jonh Wiley and Sons, New York, 1983).

[2]J. W. Christain, The Theory of Transformations in Metals and Alloys, second edition (Pergamon, Oxford, 1975).

[3]C. Zener, Phys. Rev. 71, 846 (1974); Elasticity and Anelasticity Metals, by C. Zener (Univ. of Chicago Press, Chicago, 1948).

[4]J. Friedel, J. de Physique - Lettres 35, L-59 (1974).

[5]D. J. Decker, W. A. Bassett, L. Merrill, H. T. Hall, and J. D. Barnett, J. Phys. Chem. Ref. Data 1, 773-836 (1972).

[6]K. Takemura and K. Syassen, J. Phys. F 15, 543 (1985).

[7]M. Born and K. Huang, Dynamical Theory of Crystal Lattice (Oxford University Press, London, 1956).

[8]A. A. Maradudin, E. W. Montroll, G. H. Weiss, and I. P. Ipatova, Theory of Lattice Dynamics in the Harmonic Approximation (Academic, New York, 1971).

[9]G. Venkataraman, L. A. Feldkamp, and V. C. Sahni, Dynamics of Perfect Crystals (MIT Press, Cambridge, Mass., 1975).

[10]S. K. Sinha, Crit. Rev. Solid State Sci. 4, 273 (1973).

[11]S. K. Sinha, T. O. Brun, L. D. Muhlestein, and J. Sakurai, Phys. Rev. B 1, 2430 (1970).

[12]C. M. Varma and W. Weber, Phys. Rev. Lett. 39, 1094 (1977); Phys. Rev. B 19, 6142 (1979).

[13]Y. Chen, K.-M. Ho, B. N. Harmon, and C. Stassis, Phys. Rev. B 33, 3684 (1985).

[14]Y. Chen, C.-L. Fu, K.-M. Ho, and B. N. Harmon, Phys. Rev. B 31, 6775 (1985).

[15]J. Mizuki and C. Stassis, Phys. Rev. B 32, 8372 (1985).

[16]A. O. Moriarty, Phys. Rev. 161, 445 (1967).

ACKNOWLEDGMENTS

I wish to express my deepest appreciation to my advisors and thesis directors, Dr. K.-M. Ho and Dr. B. N. Harmon, for their constant help, guidance, and friendly encouragement during my stay at Iowa State, and in the accomplishment of this project.

I would like to express my gratitude to Dr. C.-L. Fu and Dr. C.-C. Chan for stimulating discussions. Collaborations with Mrs. Y.-Y. Ye and Dr. P.-A. Lindgård on phonon-phonon coupling calculations (Section V) are greatfully acknowledged. I sincerely thank the members of my thesis committee: Dr. B.-L. Young, Dr. C. Stassis, Dr. C. Ng and Dr. J.-L. Staudenmann, for their support.

I am most grateful to my wife for her consistent support during the course of this work.

I am grateful to Ames Laboratory-U. S. Department of Energy for financial support.